Atomistic simulation study of the silicon carbide precipitation in silicon

F. Zirkelbach

Lehrstuhlseminar

17. Juni 2010

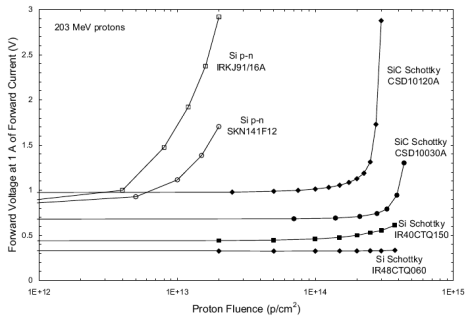

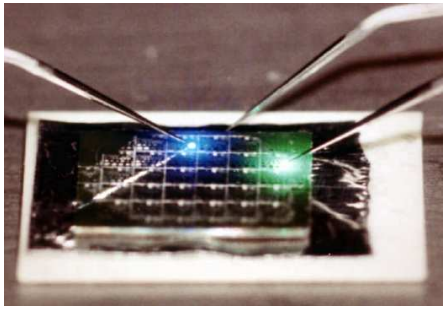

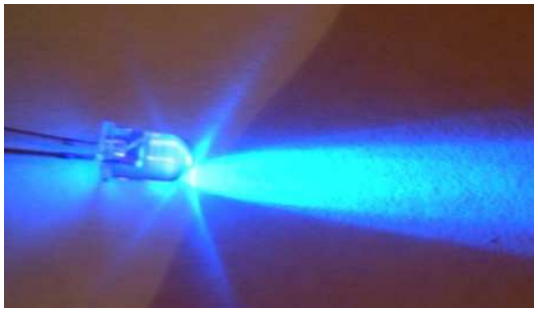

PROPERTIES

wide band gap

high electric breakdown field

good electron mobility

high electron saturation drift velocity

high thermal conductivity

hard and mechanically stable

chemically inert

radiation hardness

APPLICATIONS

high-temperature, high power
and high-frequency
electronic and optoelectronic devices

material suitable for extreme conditions
microelectromechanical systems
abrasives, cutting tools, heating elements

first wall reactor material, detectors
and electronic devices for space

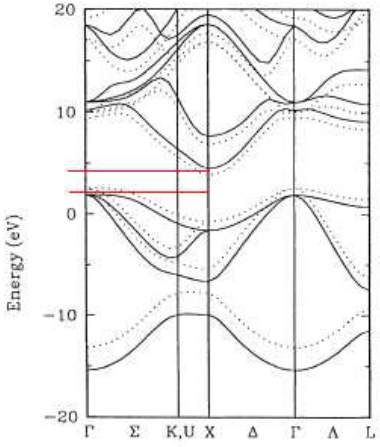

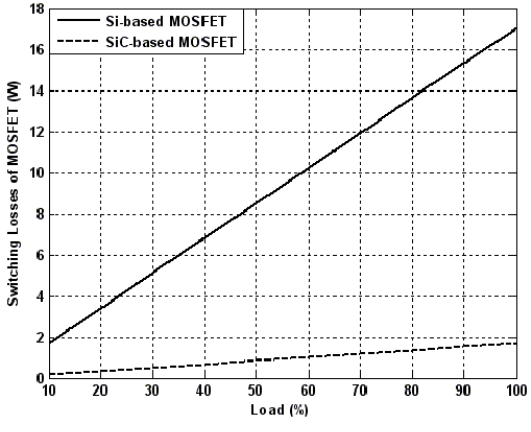

Outline

- Polytypes and fabrication of silicon carbide
- Supposed precipitation mechanism of SiC in Si
- Utilized simulation techniques
  - Molecular dynamics (MD) simulations
  - Density functional theory (DFT) calculations
- C and Si self-interstitial point defects in silicon
- Silicon carbide precipitation simulations
- Investigation of a silicon carbide precipitate in silicon
- Summary / Conclusion / Outlook

Polytypes of SiC

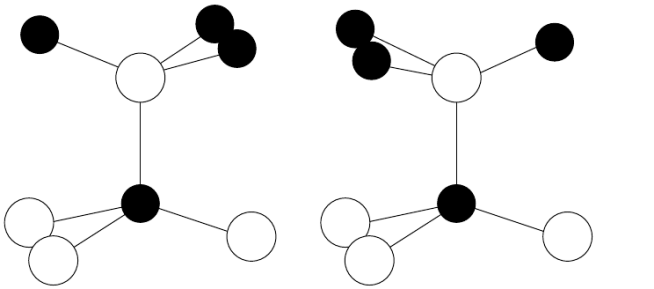

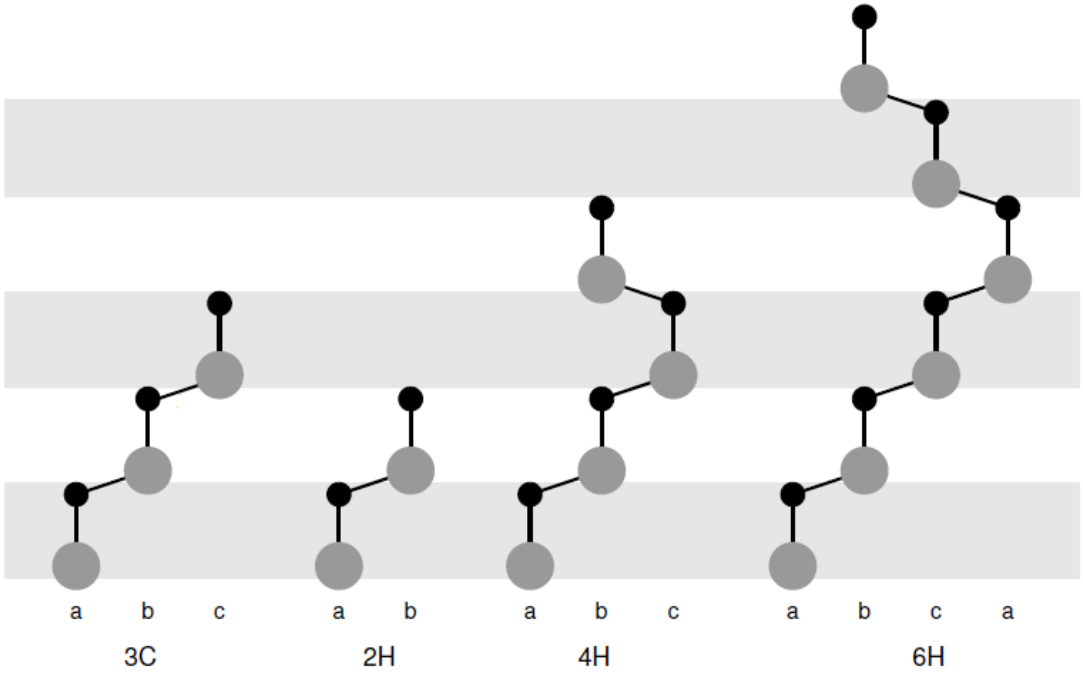

	3C-SiC	4H-SiC	6H-SiC	Si	GaN	Diamond
Hardness [Mohs]		—— 9.6 ——		6.5	-	10
Band gap [eV]	2.36	3.23	3.03	1.12	3.39	5.5
Break down field [10^6 V/cm]	4	3	3.2	0.6	5	10
Saturation drift velocity [10^7 cm/s]	2.5	2.0	2.0	1	2.7	2.7
Electron mobility [cm^2/Vs]	800	900	400	1100	900	2200
Hole mobility [cm^2/Vs]	320	120	90	420	150	1600
Thermal conductivity [W/cmK]	5.0	4.9	4.9	1.5	1.3	22

Values for $T = 300$ K

Fabrication of silicon carbide

SiC - *Born from the stars, perfected on earth.*

Conventional thin film SiC growth:

- Sublimation growth using the modified Lely method
  - SiC single-crystalline seed at $T = 1800\,^{\circ}\mathrm{C}$
  - Surrounded by polycrystalline SiC in a graphite crucible at $T = 2100 - 2400\,^{\circ}\mathrm{C}$
  - Deposition of supersaturated vapor on cooler seed crystal
- Homoepitaxial growth using CVD
  - Step-controlled epitaxy on off-oriented 6H-SiC substrates
  - $C_3H_8/SiH_4/H_2$ at $1100 - 1500\,^{\circ}\mathrm{C}$
  - Angle, temperature $\rightarrow$ 3C/6H/4H-SiC
  - High quality but limited in size of substrates
- Heteroepitaxial growth of 3C-SiC on Si using CVD/MBE
  - Two steps: carbonization and growth
  - $T = 650 - 1050\,^{\circ}\mathrm{C}$
  - Quality and size not yet sufficient

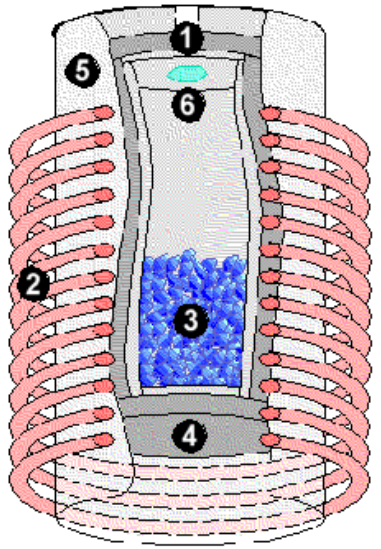

1. Lid
2. Heating
3. Source
4. Crucible
5. Insulation
6. Seed crystal

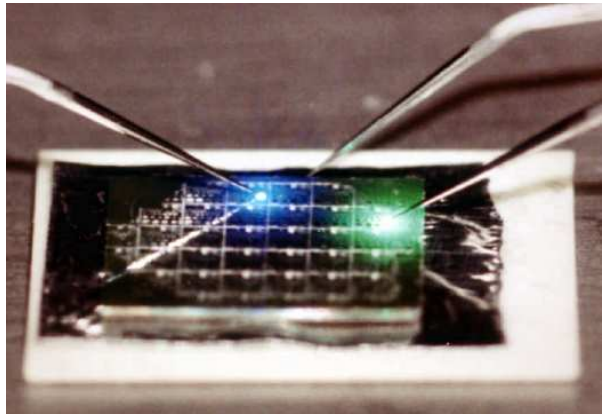

NASA: 6H-SiC and 3C-SiC LED on 6H-SiC substrate

Hex: micropipes along c-axis

3C-SiC fabrication less advanced

Fabrication of silicon carbide

Alternative approach: Ion beam synthesis (IBS) of burried 3C-SiC layers in Si(1 0 0)

- Implantation step 1
  180 keV C^+, $D = 7.9 \times 10^{17}$ cm^{-2}, $T_i = 500\,^\circ$C
  $\Rightarrow$ box-like distribution of equally sized and epitactically oriented SiC precipitates
- Implantation step 2
  180 keV C^+, $D = 0.6 \times 10^{17}$ cm^{-2}, $T_i = 250\,^\circ$C
  $\Rightarrow$ destruction of SiC nanocrystals in growing amorphous interface layers
- Annealing
  $T = 1250\,^\circ$C, $t = 10$ h
  $\Rightarrow$ homogeneous, stoichiometric SiC layer with sharp interfaces

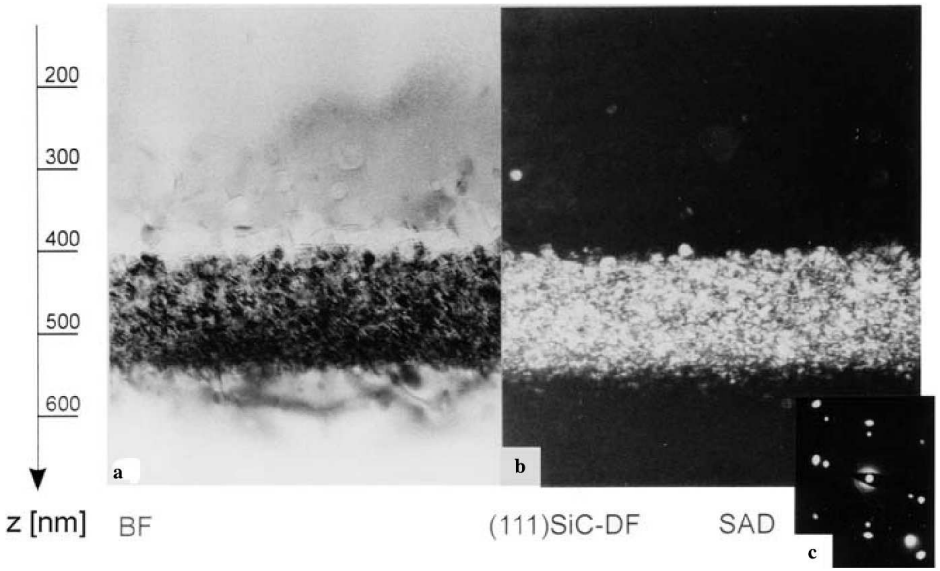

XTEM micrograph of single crystalline 3C-SiC in Si(1 0 0)

Precipitation mechanism not yet fully understood!

Understanding the SiC precipitation

$\Rightarrow$ significant technological progress in SiC thin film formation

$\Rightarrow$ perspectives for processes relying upon prevention of SiC precipitation

Supposed precipitation mechanism of SiC in Si

Si & SiC lattice structure

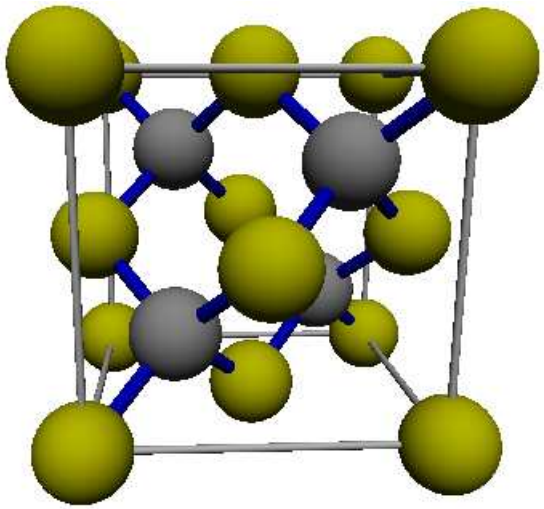

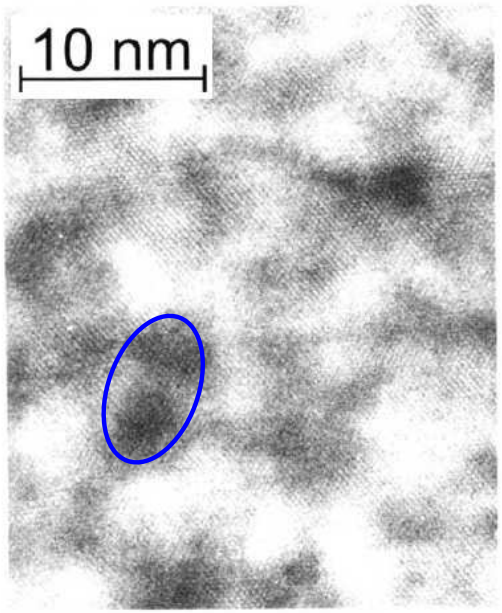

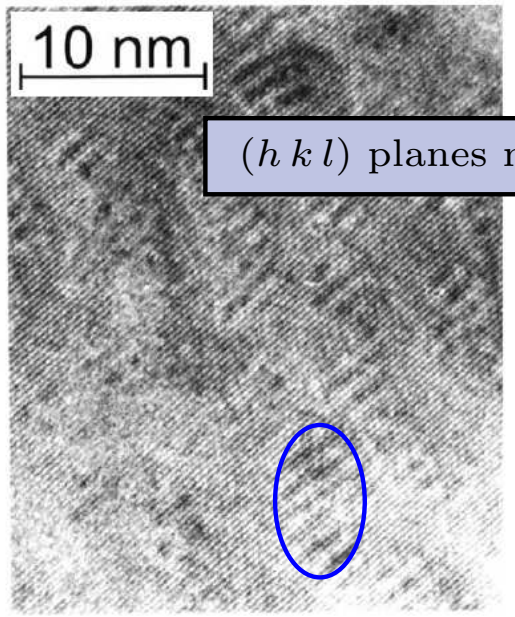

C-Si dimers (dumbbells)
on Si interstitial sites

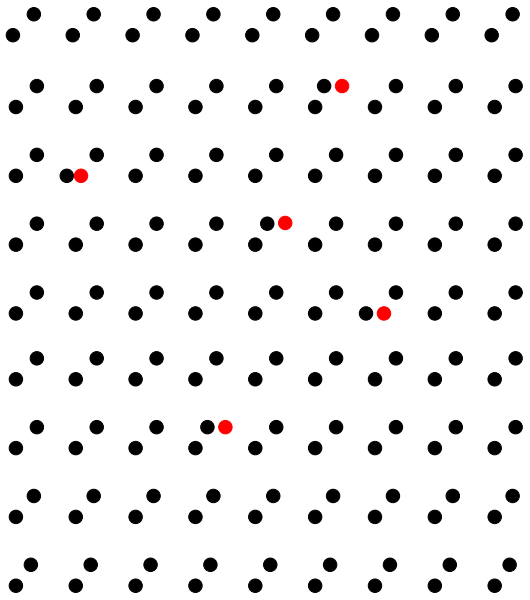

Agglomeration of C-Si dumbbells
⇒ dark contrasts

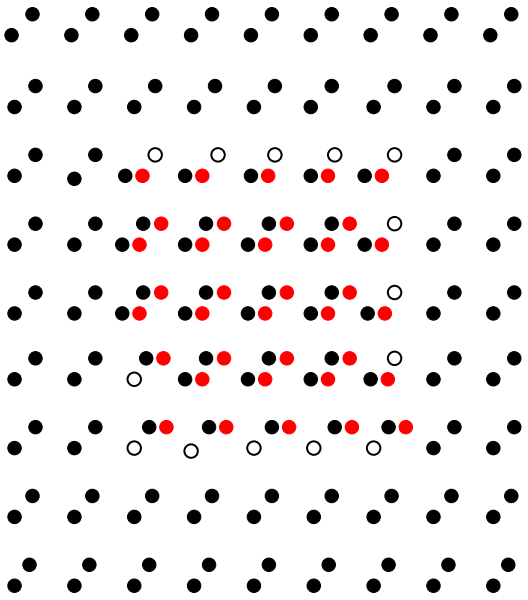

Precipitation of 3C-SiC in Si
⇒ Moiré fringes
& release of Si self-interstitials

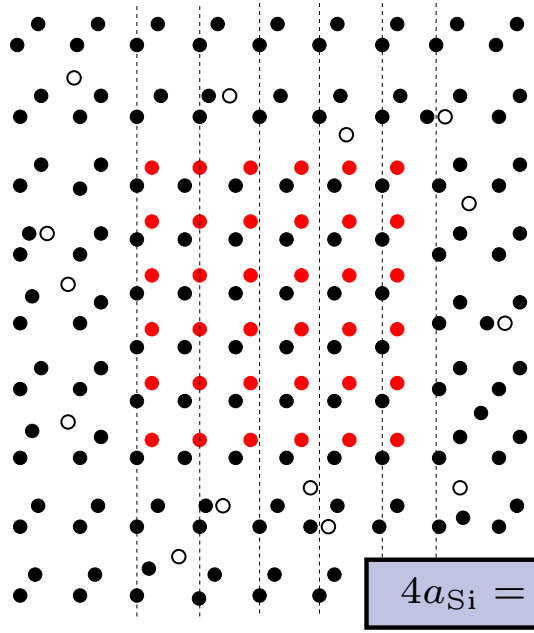

Molecular dynamics (MD) simulations

MD basics:

- Microscopic description of N particle system
- Analytical interaction potential
- Numerical integration using Newtons equation of motion as a propagation rule in 6N-dimensional phase space
- Observables obtained by time and/or ensemble averages

Details of the simulation:

- Integration: Velocity Verlet, timestep: 1 fs
- Ensemble: NpT (isothermal-isobaric)
  - Berendsen thermostat: $\tau_{\mathrm{T}} = 100$ fs
  - Berendsen barostat:
    $\tau_{\mathrm{P}} = 100$ fs, $\beta^{-1} = 100$ GPa
- Erhart/Albe potential: Tersoff-like bond order potential

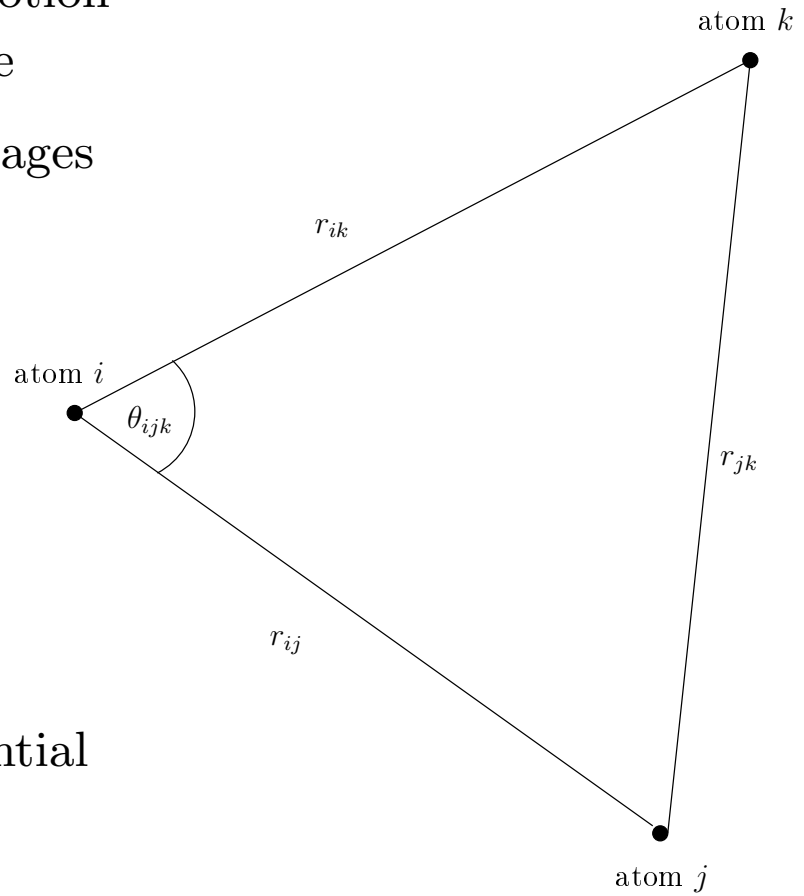

$$E = \frac{1}{2}\sum_{i \neq j} \mathcal{V}_{ij}, \quad \mathcal{V}_{ij} = f_C(r_{ij})\left[f_R(r_{ij}) + b_{ij} f_A(r_{ij})\right]$$

Density functional theory (DFT) calculations

Basic ingredients necessary for DFT

- Hohenberg-Kohn theorem - ground state density $n_0(r)$ ...
  - ... uniquely determines the ground state potential / wavefunctions
  - ... minimizes the systems total energy
- Born-Oppenheimer - N moving electrons in an external potential of static nuclei

$$H\Psi = \left[-\sum_i^N \frac{\hbar^2}{2m}\nabla_i^2 + \sum_i^N V_{\text{ext}}(r_i) + \sum_{i<j}^N V_{e-e}(r_i, r_j) \right] \Psi = E\Psi$$

- Effective potential - averaged electrostatic potential & exchange and correlation

$$V_{\text{eff}}(r) = V_{\text{ext}}(r) + \int \frac{e^2 n(r')}{|r - r'|} d^3r' + V_{\text{XC}}[n(r)]$$

- Kohn-Sham system - Schrödinger equation of N non-interacting particles

$$\left[-\frac{\hbar^2}{2m}\nabla^2 + V_{\text{eff}}(r) \right] \Phi_i(r) = \epsilon_i \Phi_i(r) \quad \Rightarrow \quad n(r) = \sum_i^N |\Phi_i(r)|^2$$

- Self-consistent solution
  $n(r)$ depends on Φ_i, which depend on V_{eff}, which in turn depends on $n(r)$
- Variational principle - minimize total energy with respect to $n(r)$

Density functional theory (DFT) calculations

Details of applied DFT calculations in this work

- Exchange correlation functional - approximations for the inhomogeneous electron gas
  - LDA: $E_{\mathrm{XC}}^{\mathrm{LDA}}[n] = \int \epsilon_{\mathrm{XC}}(n) n(r) d^3r$
  - GGA: $E_{\mathrm{XC}}^{\mathrm{GGA}}[n] = \int \epsilon_{\mathrm{XC}}(n, \nabla n) n(r) d^3r$
- Plane wave basis set - approximation of the wavefunction Φ_i by plane waves φ_j

$$\rightarrow \text{Fourier series: } \Phi_i = \sum_{|G+k|<G_{\mathrm{cut}}} c_j^i \varphi_j(r), \quad E_{\mathrm{cut}} = \frac{\hbar^2}{2m} G_{\mathrm{cut}}^2 \qquad (300 \text{ eV})$$

- Brillouin zone sampling - Γ-point only calculations
- Pseudo potential - consider only the valence electrons
- Code - VASP 4.6

MD and structural optimization

- MD integration: Gear predictor corrector algorithm
- Pressure control: Parrinello-Rahman pressure control
- Structural optimization: Conjugate gradient method

C and Si self-interstitial point defects in silicon

Procedure:

- Creation of c-Si simulation volume
- Periodic boundary conditions
- $T = 0$ K, $p = 0$ bar

↓

Insertion of interstitial C/Si atoms

↓

Relaxation / structural energy minimization

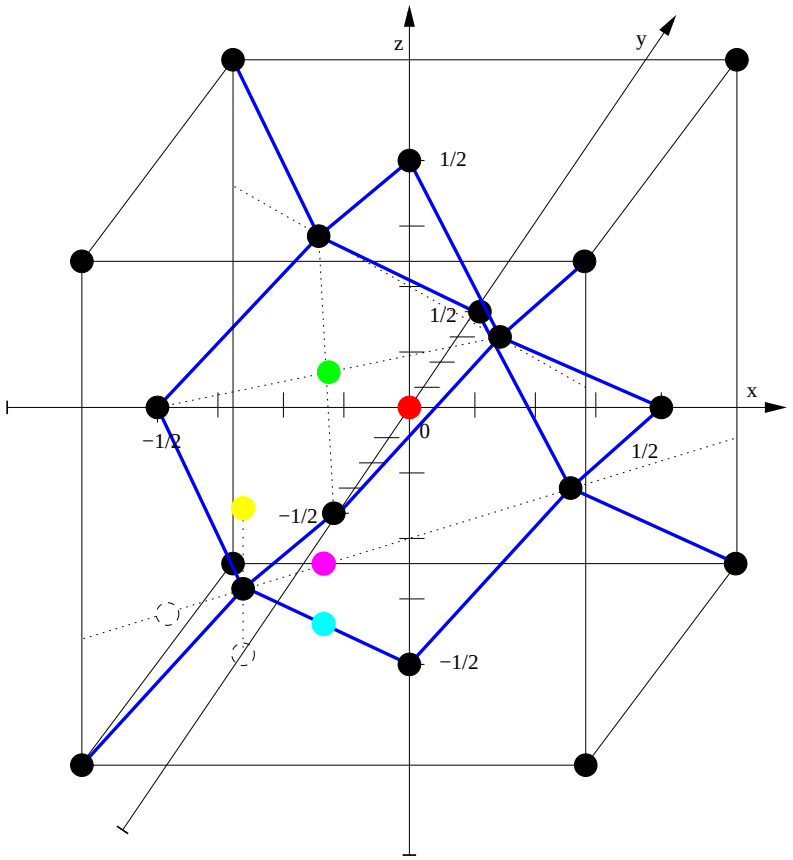

- Tetrahedral
- Hexagonal
- $\langle 1\,0\,0 \rangle$ dumbbell
- $\langle 1\,1\,0 \rangle$ dumbbell
- Bond-centered
- Vacancy / Substitutional

	size [unit cells]	# atoms
VASP	$3 \times 3 \times 3$	216 ± 1
Erhart/Albe	$9 \times 9 \times 9$	5832 ± 1

Si self-interstitial point defects in silicon

E_f [eV]	⟨1 1 0⟩ DB	H	T	⟨1 0 0⟩ DB	V
VASP	<u>3.39</u>	3.42	3.77	4.41	3.63
Erhart/Albe	4.39	4.48*	<u>3.40</u>	5.42	3.13

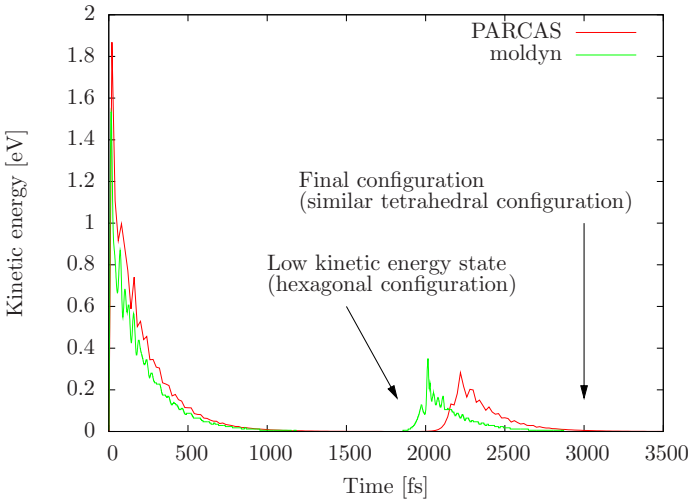

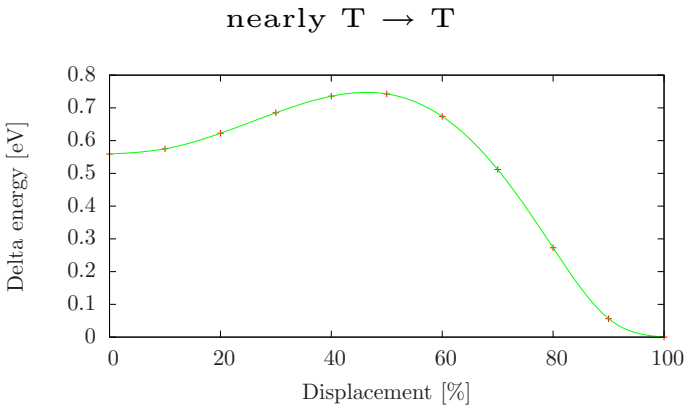

<u>⟨1 1 0⟩ dumbbell</u>

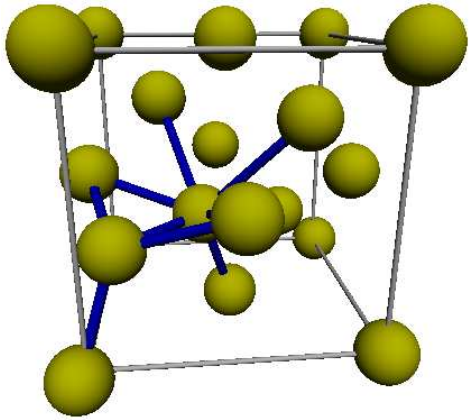

<u>Tetrahedral</u>

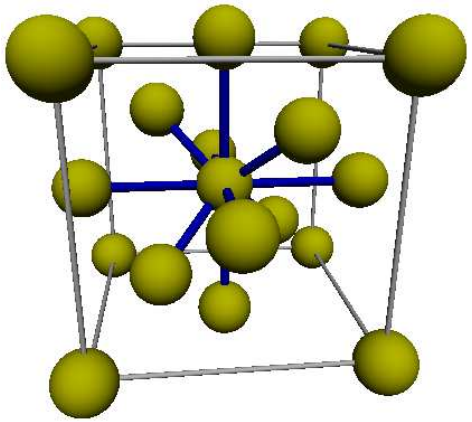

<u>Hexagonal</u> ▷

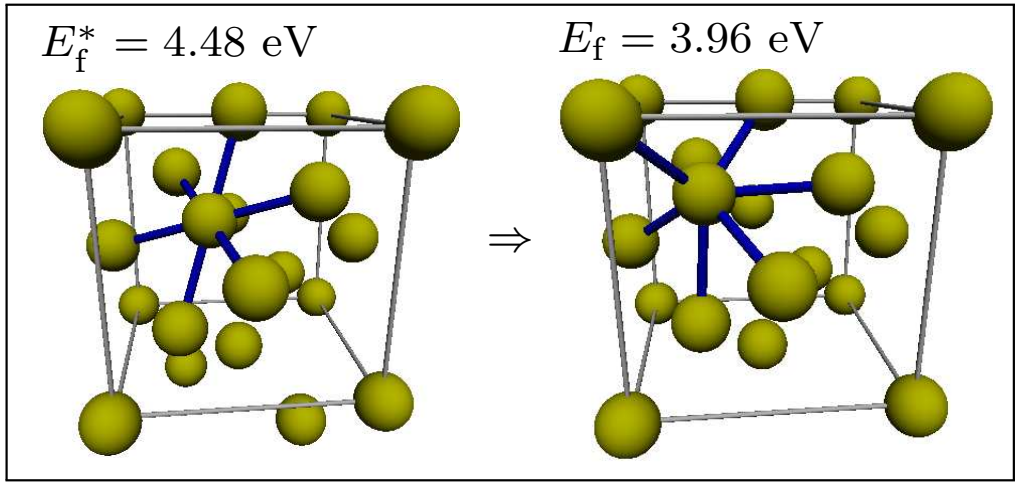

<u>Vacancy</u>

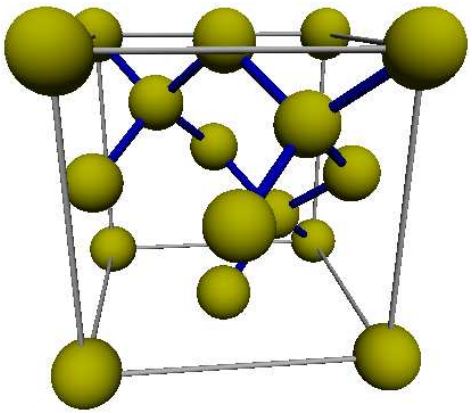

<u>⟨1 0 0⟩ dumbbell</u>

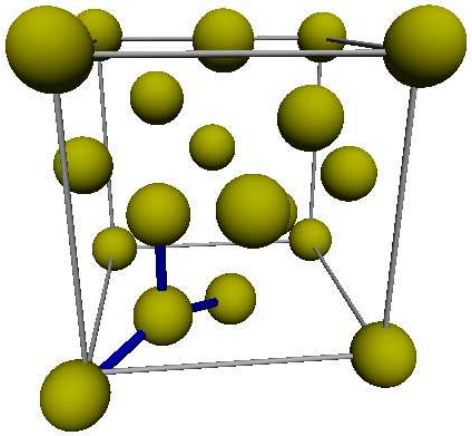

C interstitial point defects in silicon

E_f	T	H	$\langle 1\,0\,0\rangle$ DB	$\langle 1\,1\,0\rangle$ DB	S	B
VASP	unstable	unstable	3.72	4.16	1.95	4.66
Erhart/Albe MD	6.09	9.05*	3.88	5.18	0.75	5.59*

Hexagonal $\triangleright$
$E_\mathrm{f}^* = 9.05$ eV

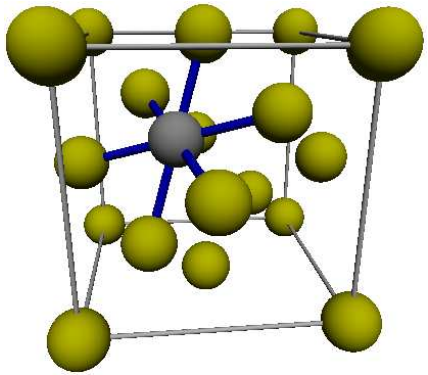

$\Rightarrow$

$\langle 1\,0\,0\rangle$
$E_\mathrm{f} = 3.88$ eV

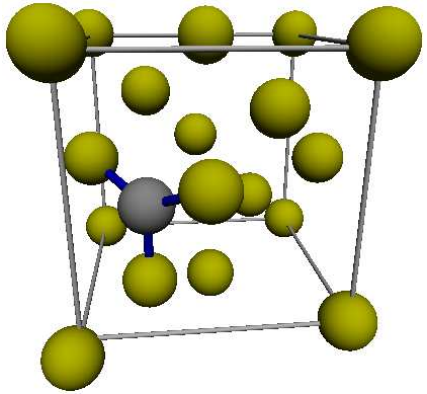

Tetrahedral

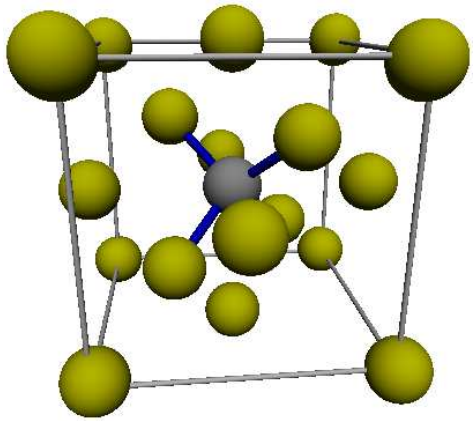

Bond-centered
$E_\mathrm{f}^* = 5.59$ eV

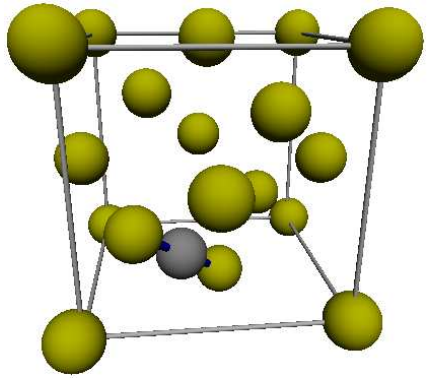

$\Rightarrow$

$\langle 1\,1\,0\rangle$ dumbbell
$E_\mathrm{f} = 5.18$ eV

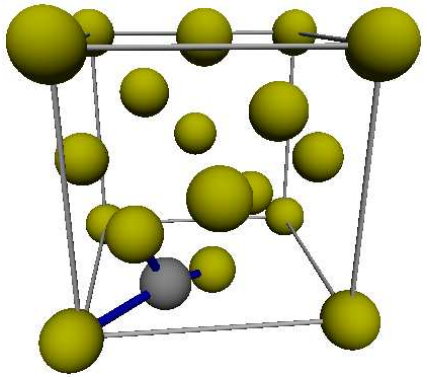

Substitutional

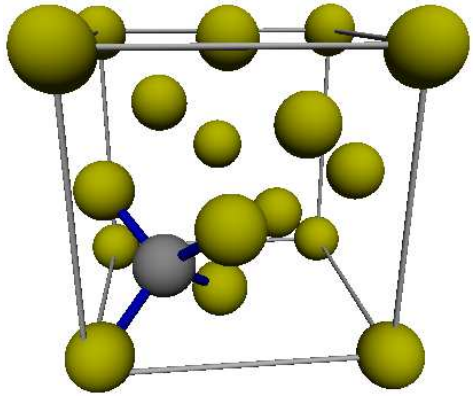

C ⟨1 0 0⟩ dumbbell interstitial configuration

Distances [nm]	$r(1C)$	$r(2C)$	$r(3C)$	$r(12)$	$r(13)$	$r(34)$	$r(23)$	$r(25)$
Erhart/Albe	0.175	0.329	0.186	0.226	0.300	0.343	0.423	0.425
VASP	0.174	0.341	0.182	0.229	0.286	0.347	0.422	0.417

Angles [°]	θ_1	θ_2	θ_3	θ_4
Erhart/Albe	140.2	109.9	134.4	112.8
VASP	130.7	114.4	146.0	107.0

Displacements [nm]	a	b	$\lvert a\rvert + \lvert b\rvert$
Erhart/Albe	0.084	-0.091	0.175
VASP	0.109	-0.065	0.174

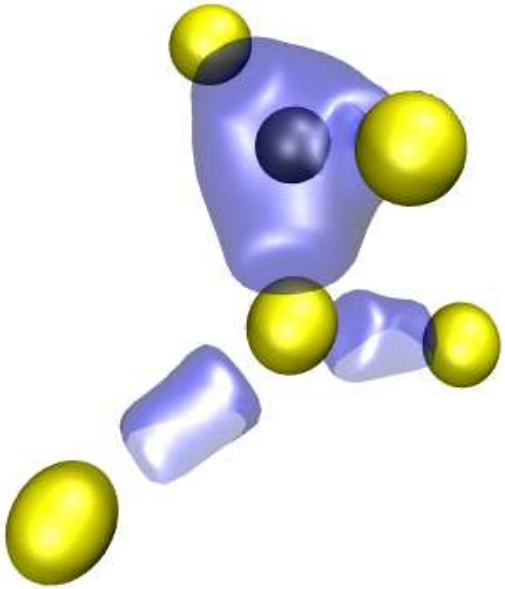

Erhart/Albe

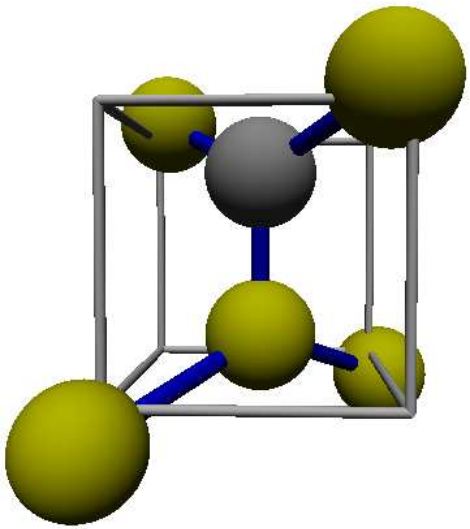

VASP

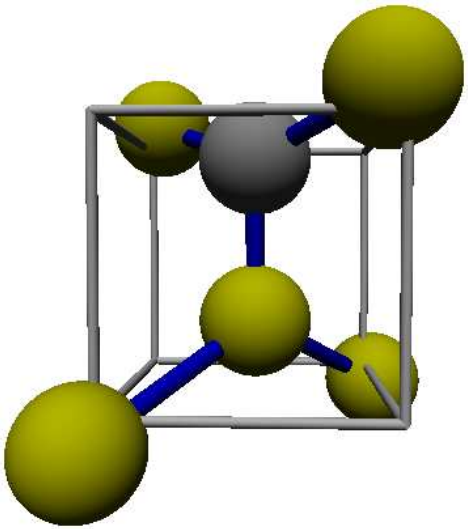

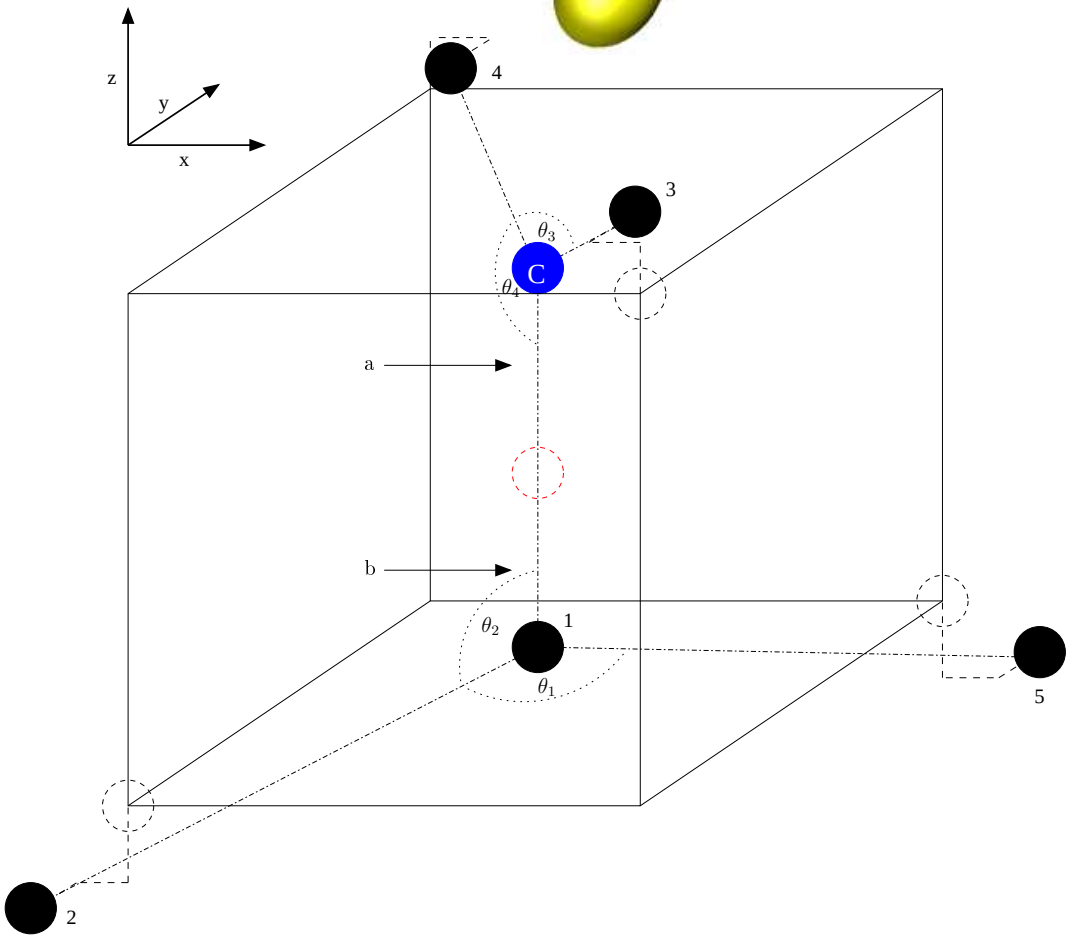

Bond-centered interstitial configuration

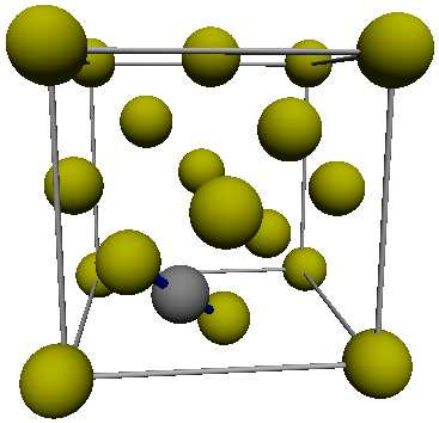

- Linear Si-C-Si bond
- Si: one C & 3 Si neighbours
- Spin polarized calculations
- No saddle point!
  Real local minimum!

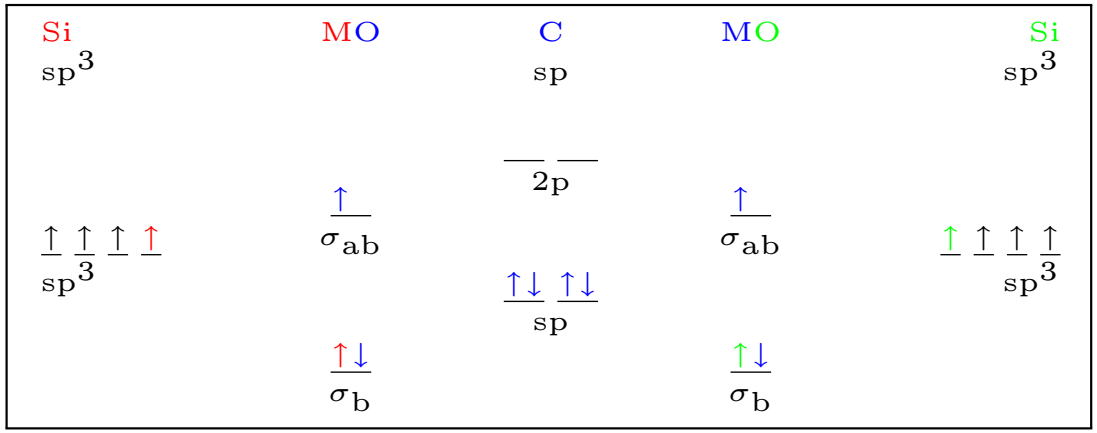

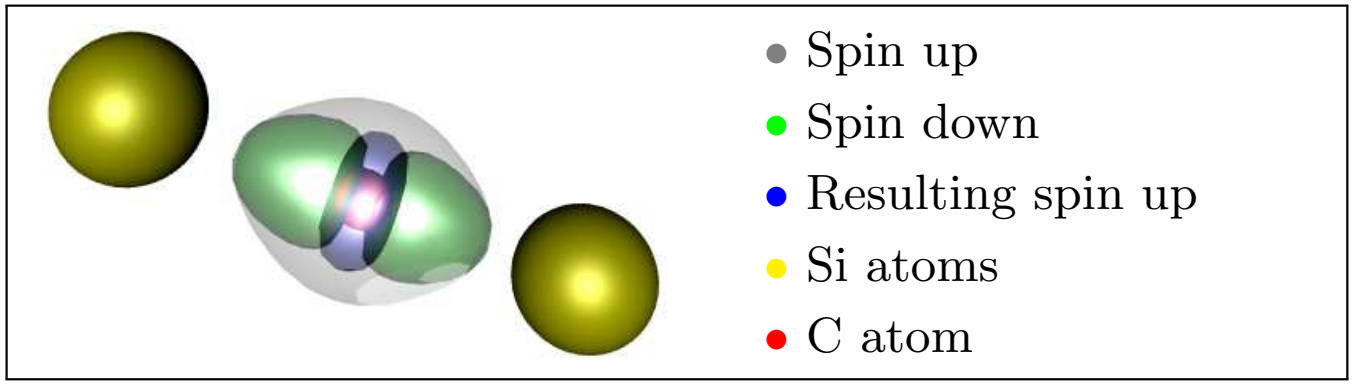

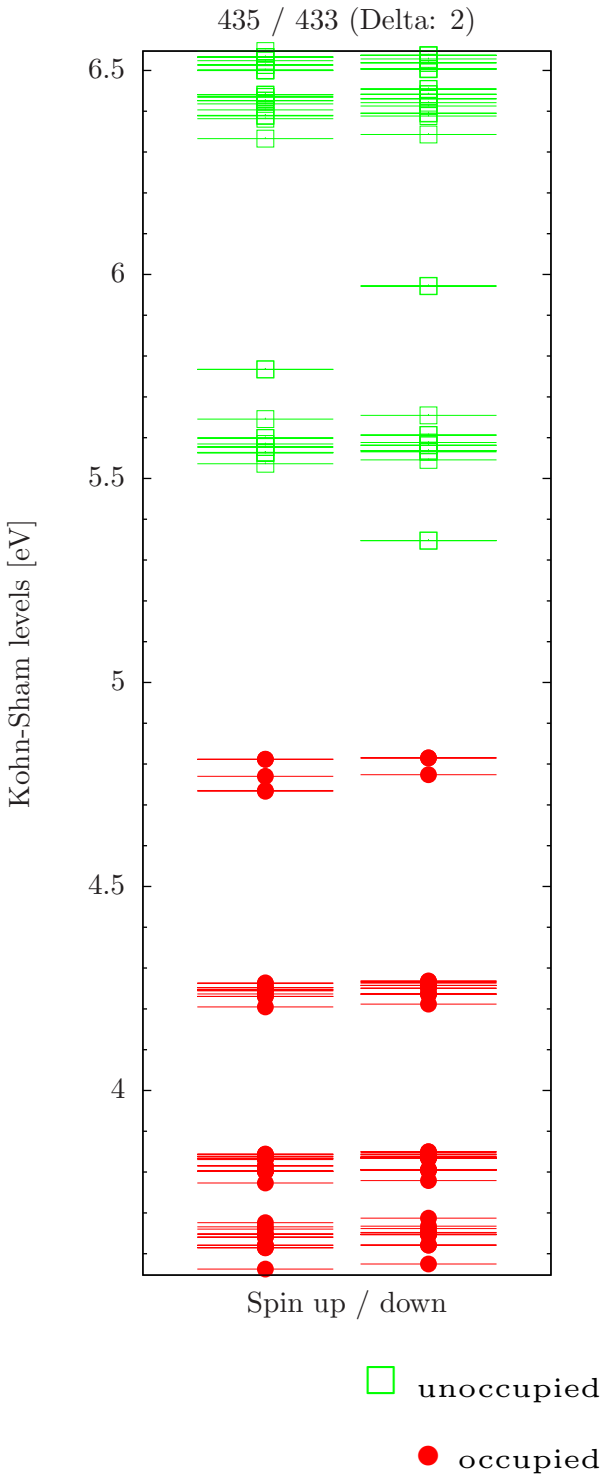

Migration of the C $\langle 1\,0\,0 \rangle$ dumbbell interstitial

Investigated pathways

$\langle 0\,0\,\bar{1} \rangle \rightarrow \langle 0\,0\,1 \rangle$

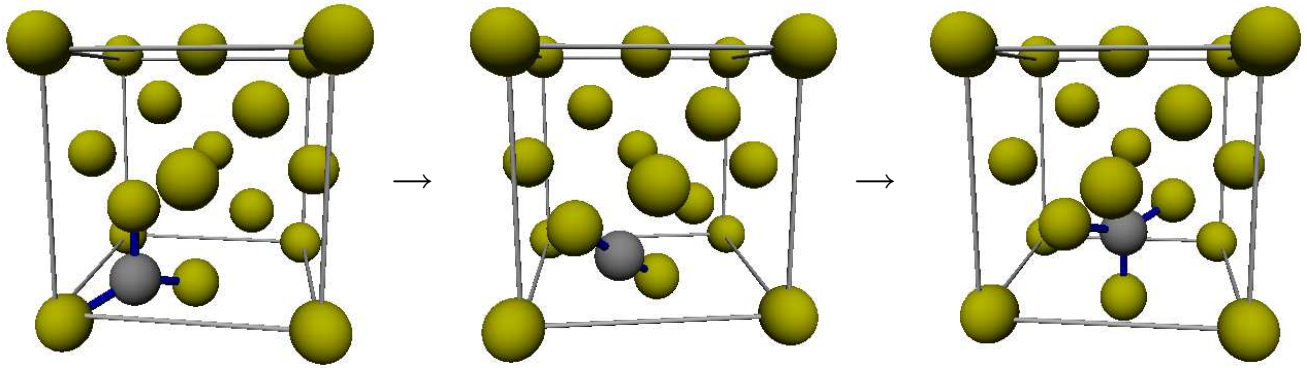

$\langle 0\,0\,\bar{1} \rangle \rightarrow \langle 0\,\bar{1}\,0 \rangle$

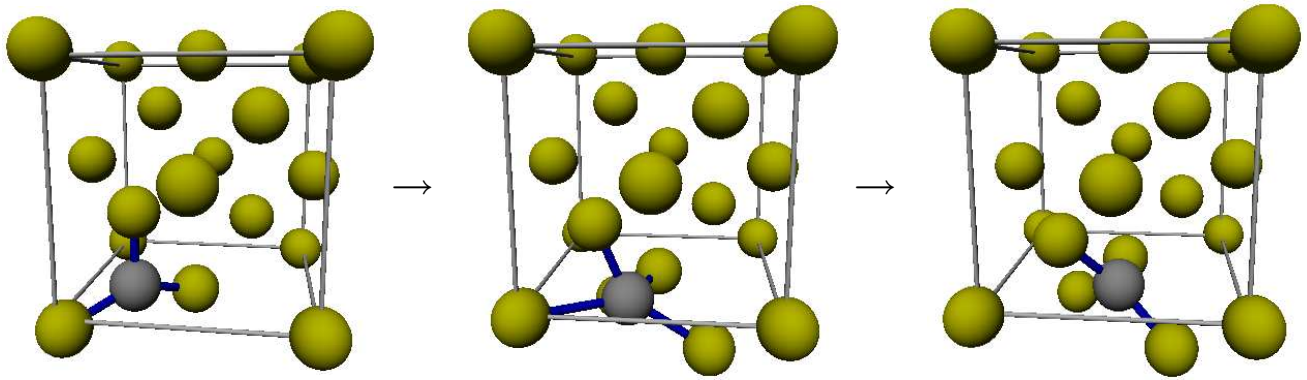

$\langle 0\,0\,\bar{1} \rangle \rightarrow \langle 0\,\bar{1}\,0 \rangle$ (in place)

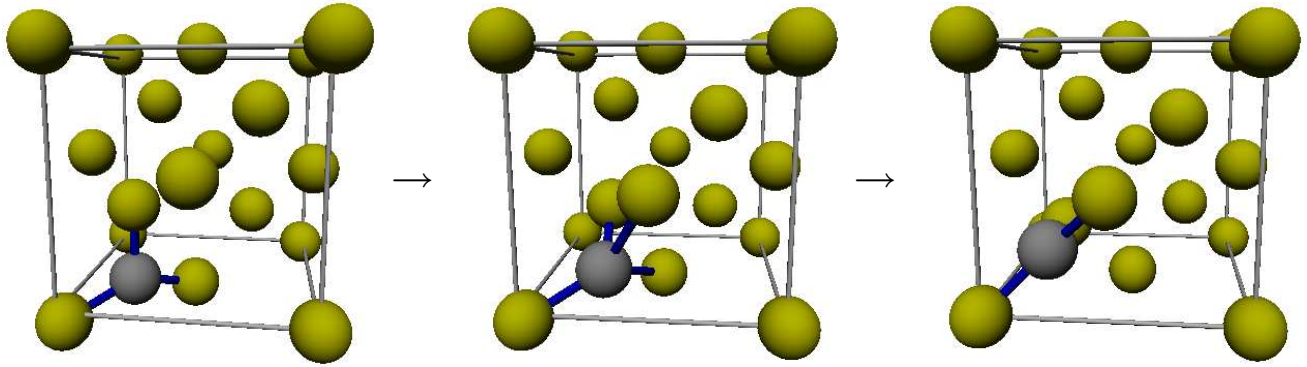

Constrained relaxation technique (CRT) method

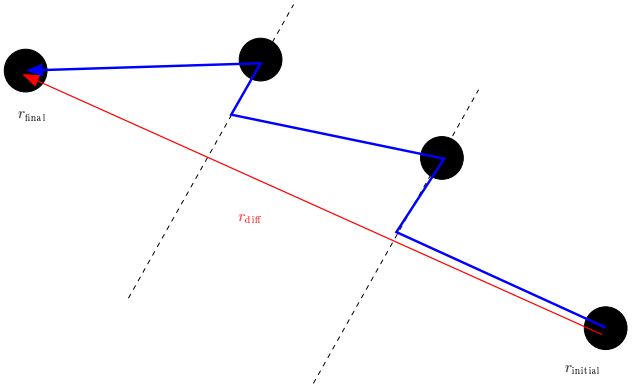

- Constrain diffusing atom
- Static constraints

Modifications

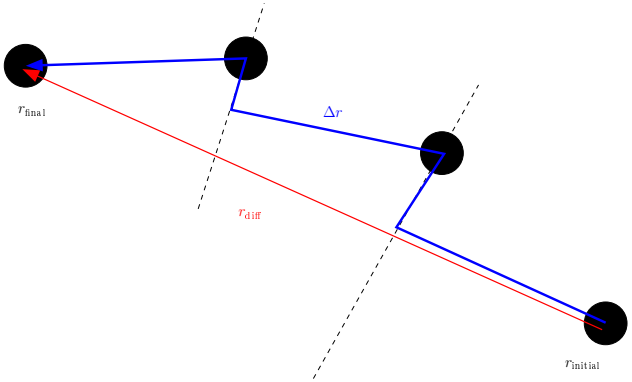

- Constrain all atoms
- Update individual constraints

Migration of the C ⟨1 0 0⟩ dumbbell interstitial

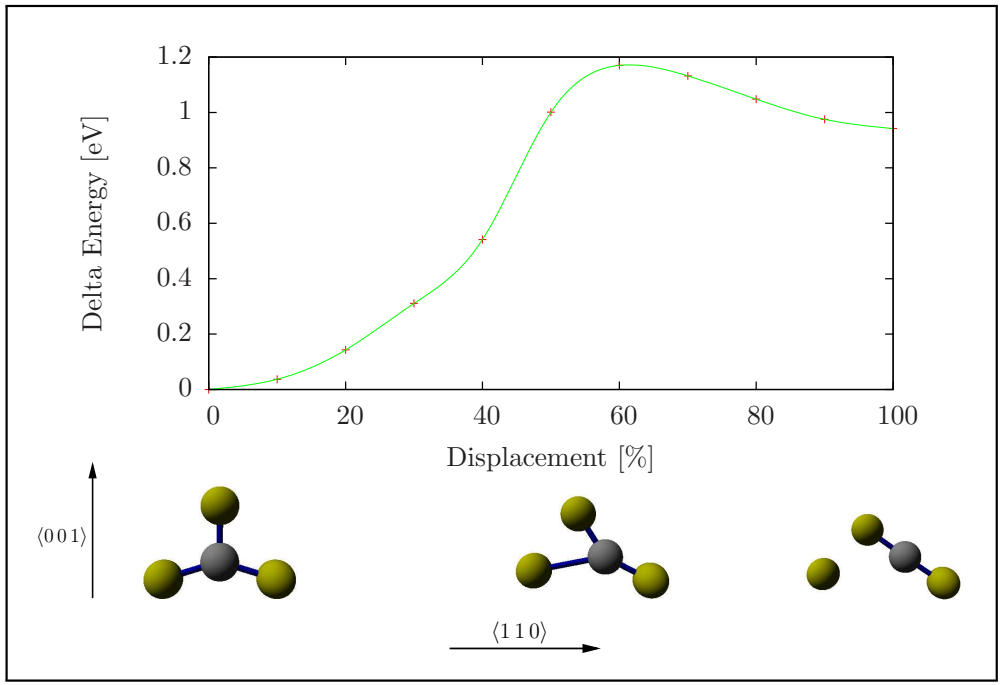

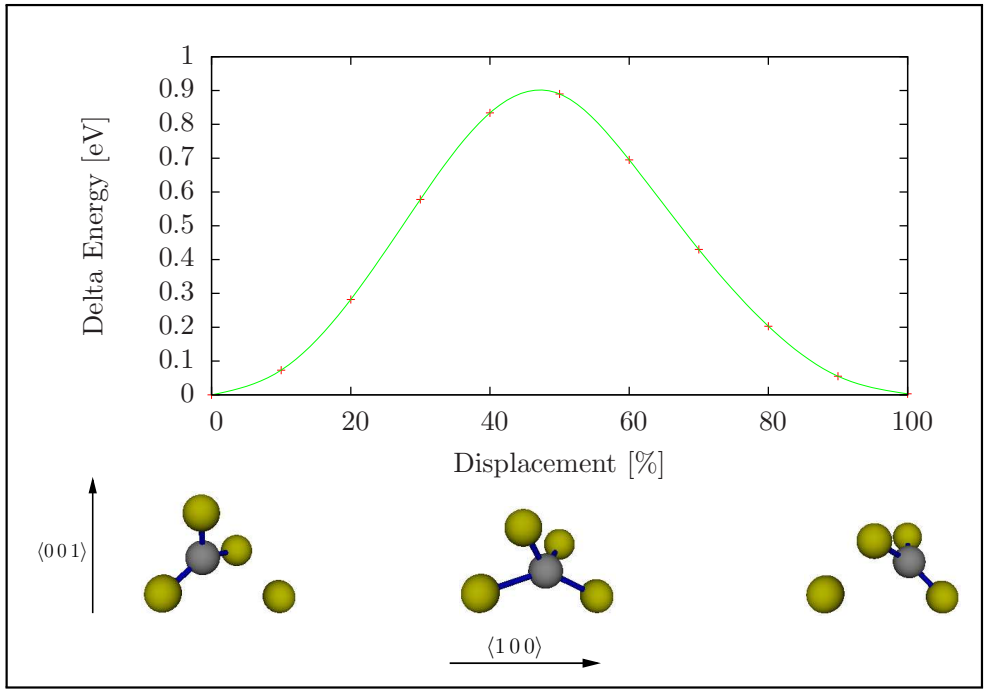

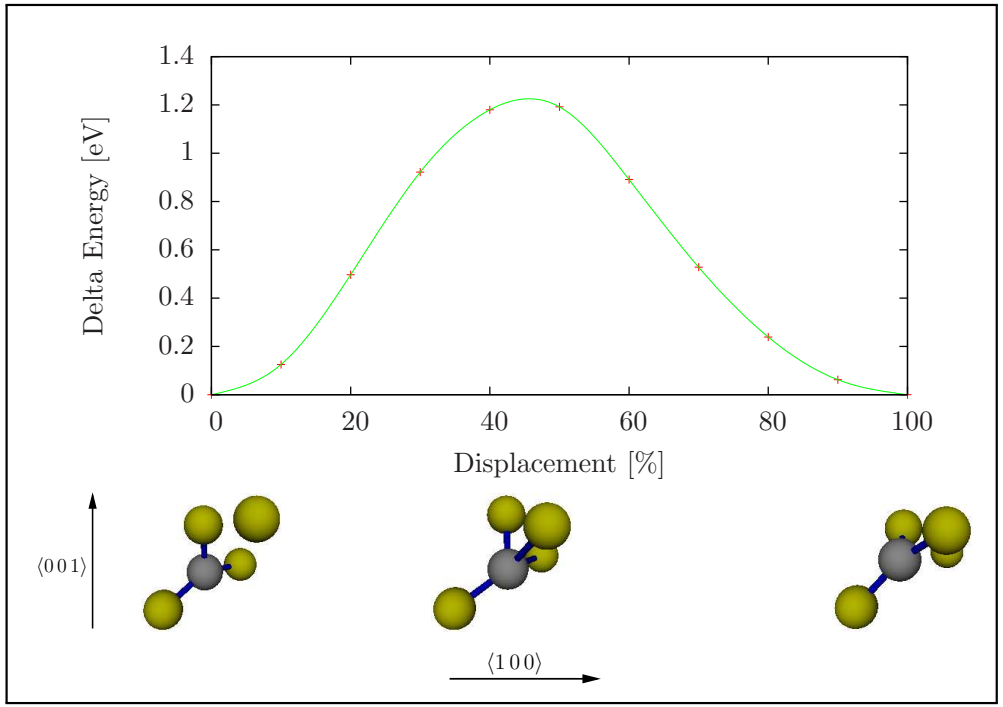

VASP results

- Energetically most favorable path
  - Path 2
  - Activation energy: ≈ 0.9 eV
  - Experimental values: 0.73 ... 0.87 eV

  ⇒ Diffusion path identified!
- Reorientation (path 3)
  - More likely composed of two consecutive steps of type 2
  - Experimental values: 0.77 ... 0.88 eV

  ⇒ Reorientation transition identified!

Migration of the C ⟨1 0 0⟩ dumbbell interstitial

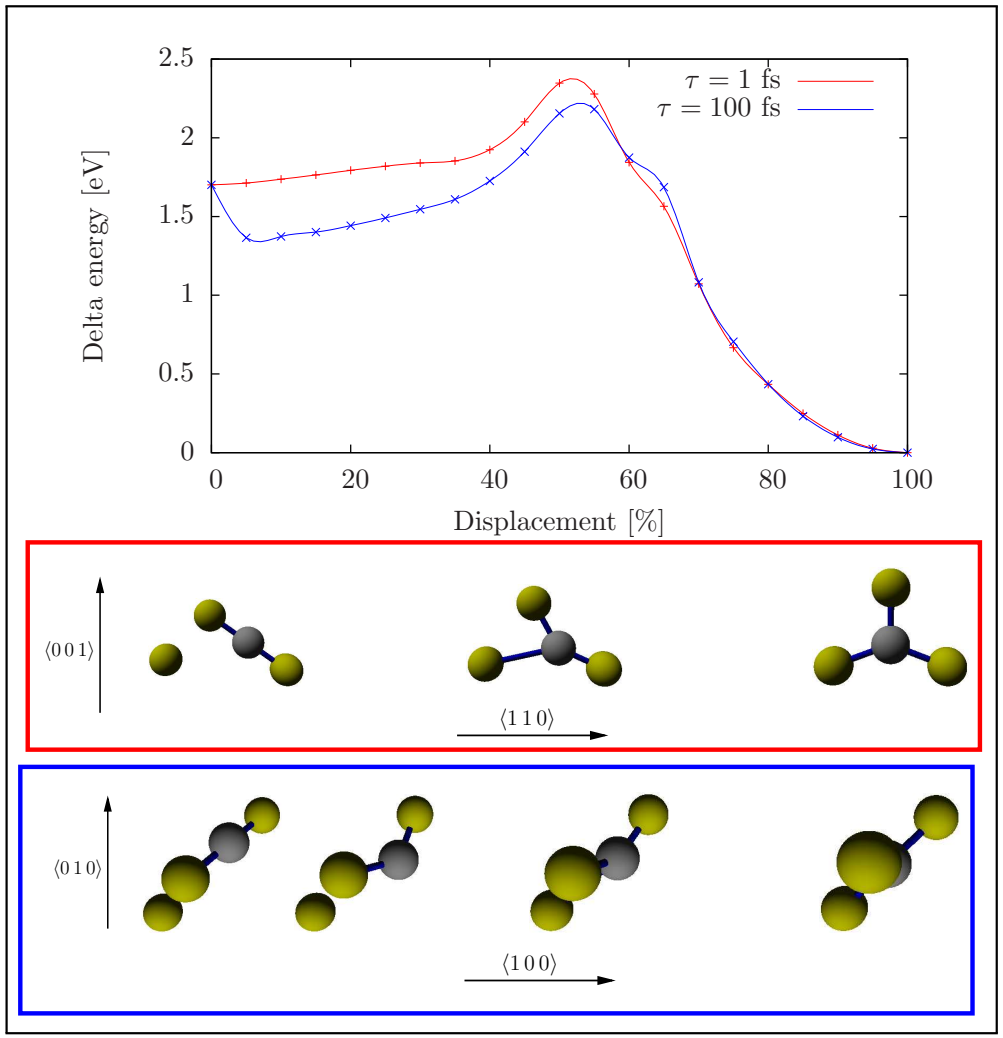

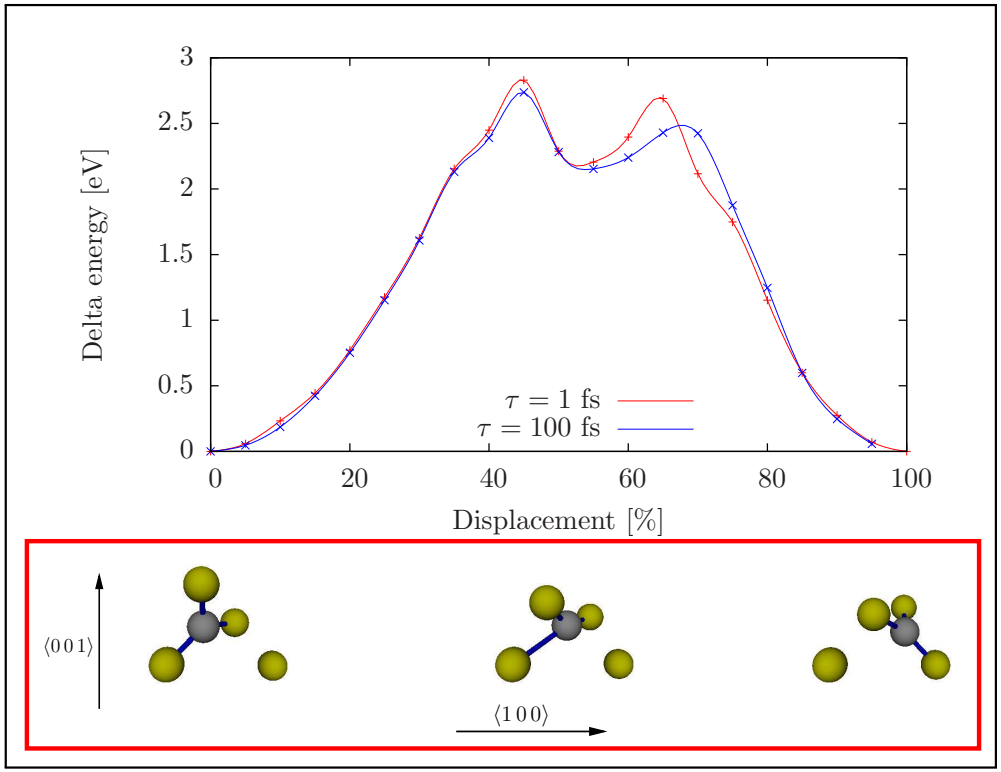

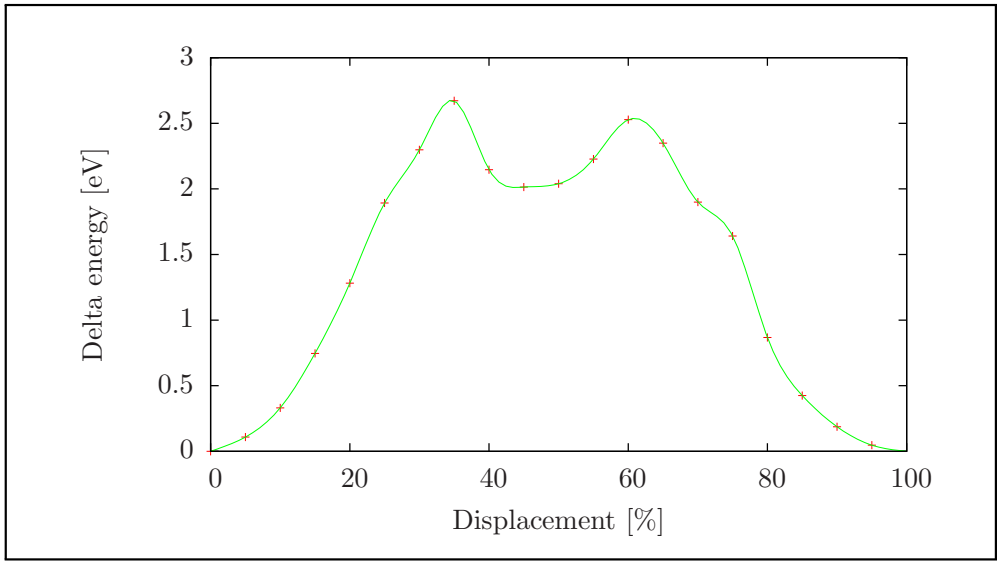

Erhart/Albe results

- Lowest activation energy: ≈ 2.2 eV
- 2.4 times higher than VASP
- Different pathway
- Transition minima (→ ⟨1 1 0⟩ dumbbell)

Migrations involving the C $\langle 1\,1\,0\rangle$ dumbbell interstitial

VASP

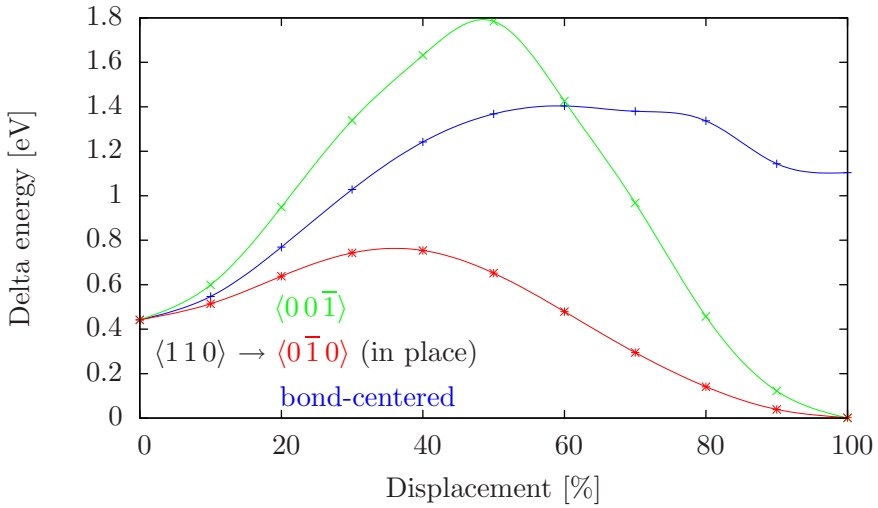

Alternative pathway and energies [eV]

$\langle 0\,\bar{1}\,0\rangle \xrightarrow{0.7} \langle 1\,1\,0\rangle \xrightarrow{0.95}$ BC $\xrightarrow{0.25} \langle 0\,0\,\bar{1}\rangle$

Composed of three single transitions

Activation energy of second transition slightly higher than direct transition (path 2)

$\Rightarrow$ very unlikely to happen

Erhart/Albe

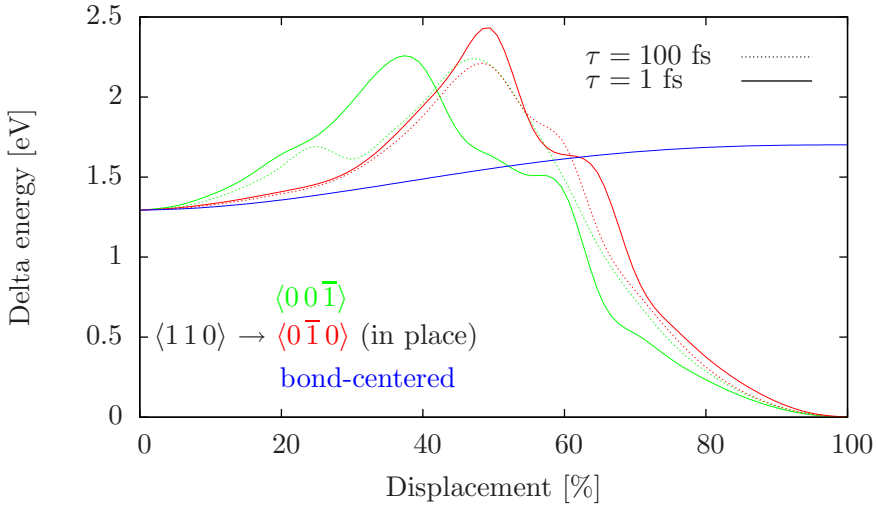

Alternative pathway and energies [eV]

$\langle 0\,0\,\bar{1}\rangle \xrightarrow{2.2} \langle 1\,1\,0\rangle \xrightarrow{0.9} \langle 0\,0\,\bar{1}\rangle$

Composed of two single transitions

Compared to direct transition: (2.2 eV & 0.5 eV)

$\Rightarrow$ more readily constituting a probable transition

Combinations with a C-Si $\langle 1\,0\,0\rangle$-type interstitial

Binding energy: $E_\mathrm{b} = E_\mathrm{f}^{\text{defect combination}} - E_\mathrm{f}^{\mathrm{C}\ \langle 0\,0\,\bar{1}\rangle\ \text{dumbbell}} - E_\mathrm{f}^{\text{2nd defect}}$

E_b [eV]	1	2	3	4	5	R
$\langle 0\,0\,\bar{1}\rangle$	-0.08	-1.15	-0.08	0.04	-1.66	-0.19
$\langle 0\,0\,1\rangle$	0.34	0.004	-2.05	0.26	-1.53	-0.19
$\langle 0\,\bar{1}\,0\rangle$	-2.39	-0.17	-0.10	-0.27	-1.88	-0.05
$\langle 0\,1\,0\rangle$	-2.25	-1.90	-2.25	-0.12	-1.38	-0.06
$\langle \bar{1}\,0\,0\rangle$	-2.39	-0.36	-2.25	-0.12	-1.88	-0.05
$\langle 1\,0\,0\rangle$	-2.25	-2.16	-0.10	-0.27	-1.38	-0.06
C substitutional ($\mathrm{C_S}$)	0.26	-0.51	-0.93	-0.15	0.49	-0.05
Vacancy	-5.39 ($\rightarrow \mathrm{C_S}$)	-0.59	-3.14	-0.54	-0.50	-0.31

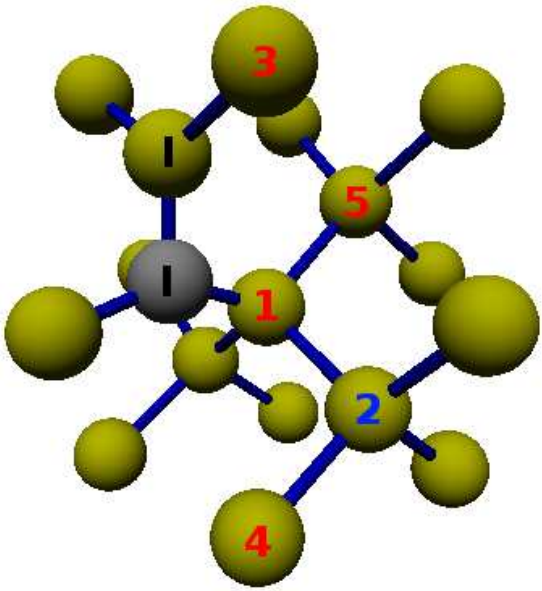

$\langle 1\,0\,0\rangle$ at position 1

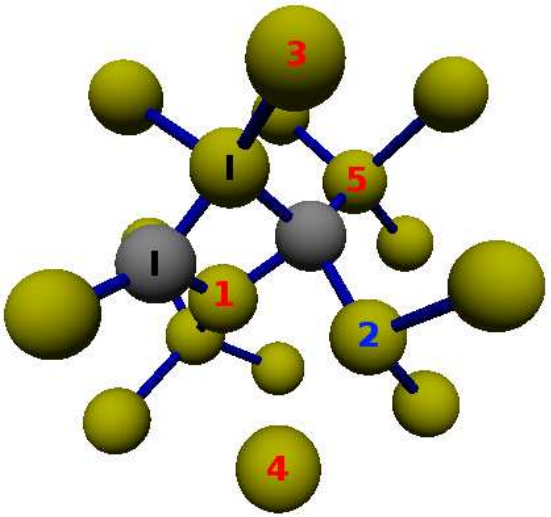

$\langle 0\,\bar{1}\,0\rangle$ at position 1

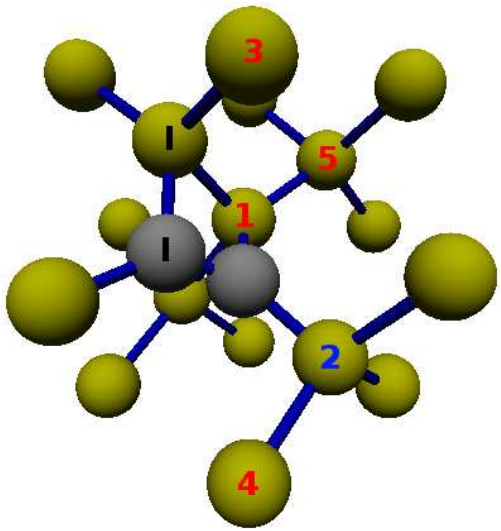

- Restricted to VASP simulations
- $E_\mathrm{b} = 0$ for isolated non-interacting defects
- $E_\mathrm{b} \rightarrow 0$ for increasing distance (R)
- Stress compensation / increase
- Most favorable: C clustering
- Unfavored: antiparallel orientations
- Indication of energetically favored agglomeration

Combinations of C-Si $\langle 1\,0\,0\rangle$-type interstitials

Energetically most favorable combinations along $\langle 1\,1\,0\rangle$

	1	2	3	4	5	6
E_b [eV]	-2.39	-1.88	-0.59	-0.31	-0.24	-0.21
C-C distance [Å]	1.4	4.6	6.5	8.6	10.5	10.8
Type	$\langle \bar{1}\,0\,0\rangle$	$\langle 1\,0\,0\rangle$	$\langle 1\,0\,0\rangle$	$\langle 1\,0\,0\rangle$	$\langle 1\,0\,0\rangle$	$\langle 1\,0\,0\rangle$, $\langle 0\,\bar{1}\,0\rangle$

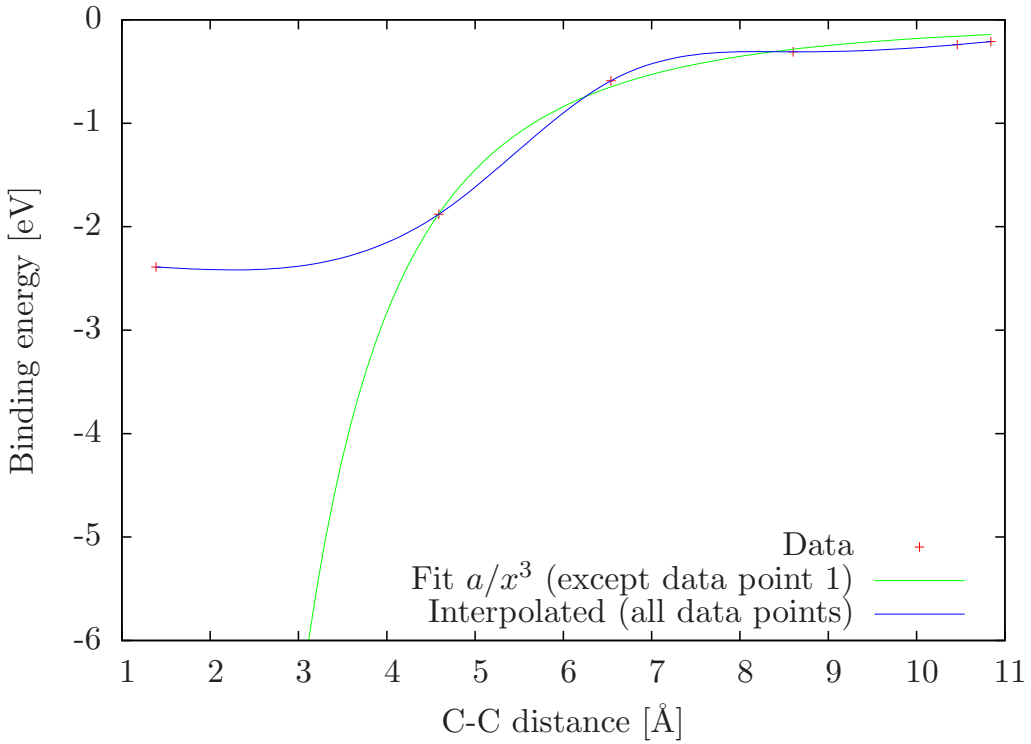

Interaction proportional to reciprocal cube of C-C distance

Saturation in the immediate vicinity

Combinations of substitutional C and ⟨1 1 0⟩ Si self-interstitials

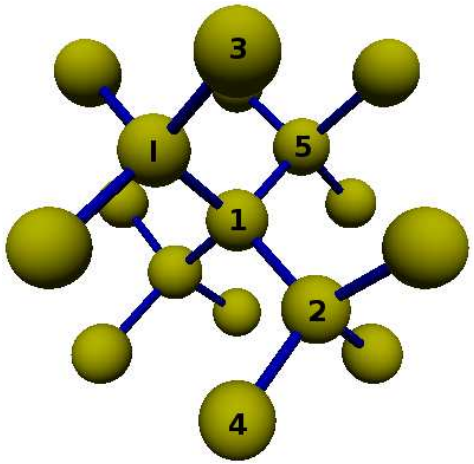

C_{sub}	⟨1 1 0⟩	⟨$\bar{1}$ 1 0⟩	⟨0 1 1⟩	⟨0 $\bar{1}$ 1⟩	⟨1 0 1⟩	⟨$\bar{1}$ 0 1⟩
1	I	III	III	I	III	I
2	II	A	A	II	C	V
3	III	I	III	I	I	III
4	IV	B	D	E	E	D
5	V	C	A	II	A	II

Conf	I	II	III	IV	V	A	B	C	D	E
E_f [eV]	4.37	5.26	5.57	5.37	5.12	5.10	5.32	5.28	5.39	5.32
E_b [eV]	-0.97	-0.08	0.22	-0.02	-0.23	-0.25	-0.02	-0.06	0.05	-0.03
r [nm]	0.292	0.394	0.241	0.453	0.407	0.408	0.452	0.392	0.456	0.453

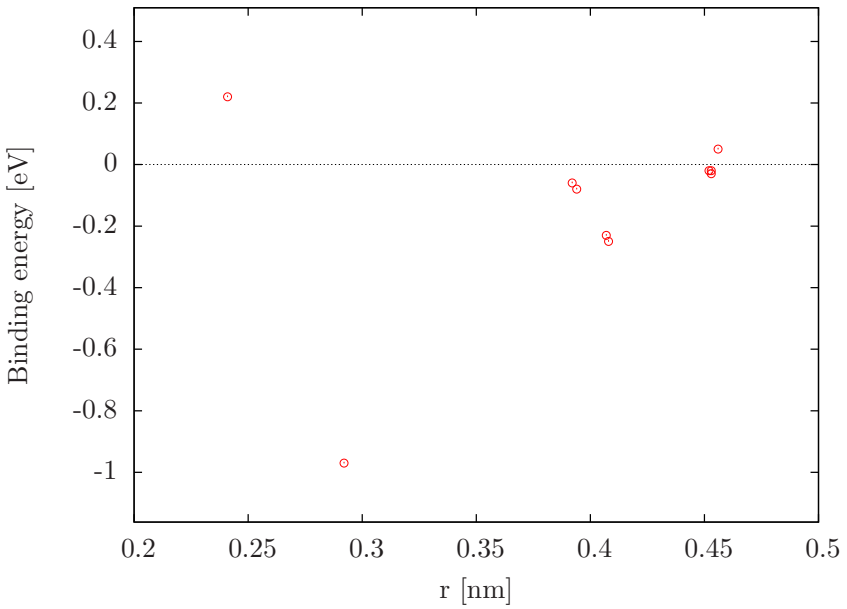

- IBS: C may displace Si
  ⇒ C_{sub} + ⟨1 1 0⟩ Si self-interstitial
- Assumption:
  ⟨1 1 0⟩-type → favored combination

⇒ Less favorable than C-Si ⟨1 0 0⟩ dumbbell
($E_f = 3.88$ eV)

⇒ Interaction drops quickly to zero
(low interaction capture radius)

Migration in C-Si $\langle 1\,0\,0 \rangle$ and vacancy combinations

Pos 2, $E_\mathrm{b} = -0.59$ eV

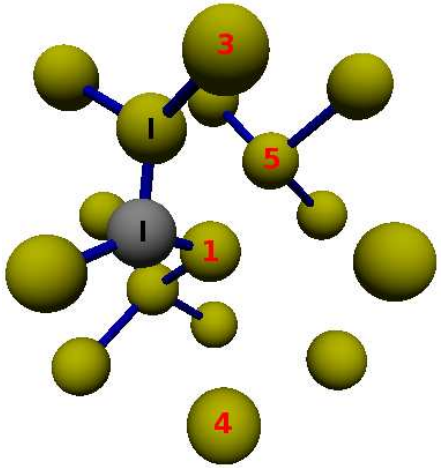

Low activation energies

High activation energies for reverse processes

$\Downarrow$

C_{sub} very stable

Without nearby $\langle 1\,1\,0 \rangle$ Si self-interstitial (IBS)

$\Downarrow$

Formation of SiC by successive substitution by C

Pos 3, $E_\mathrm{b} = -3.14$ eV

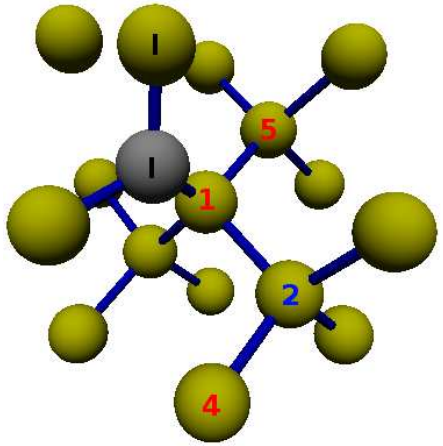

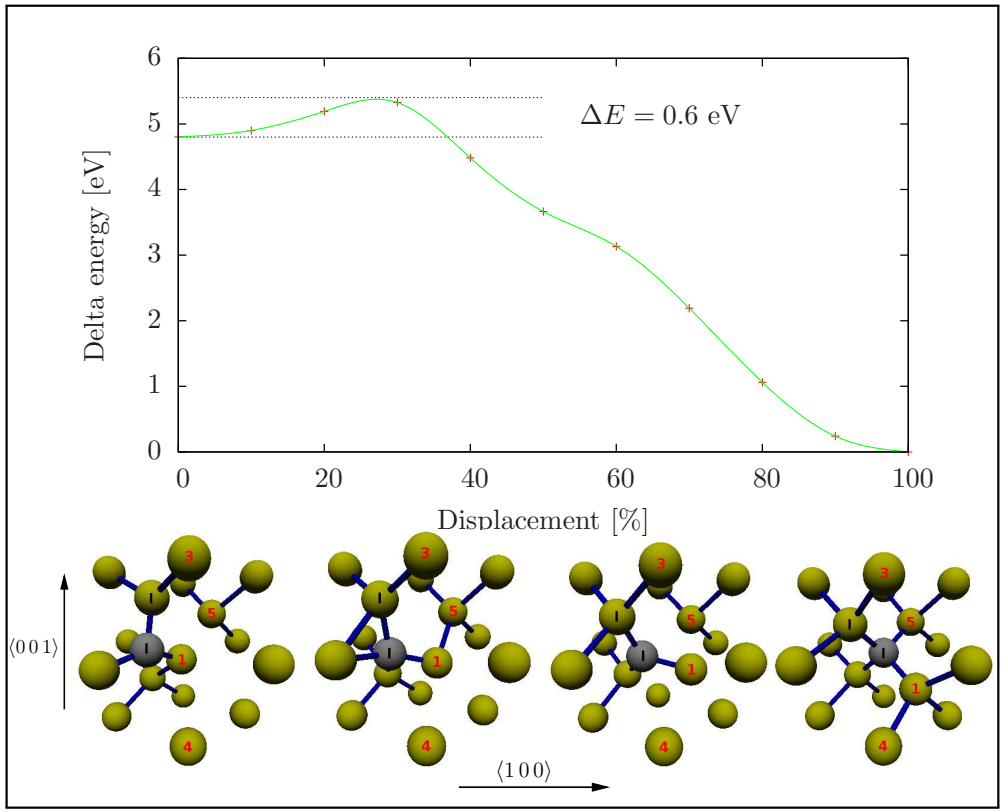

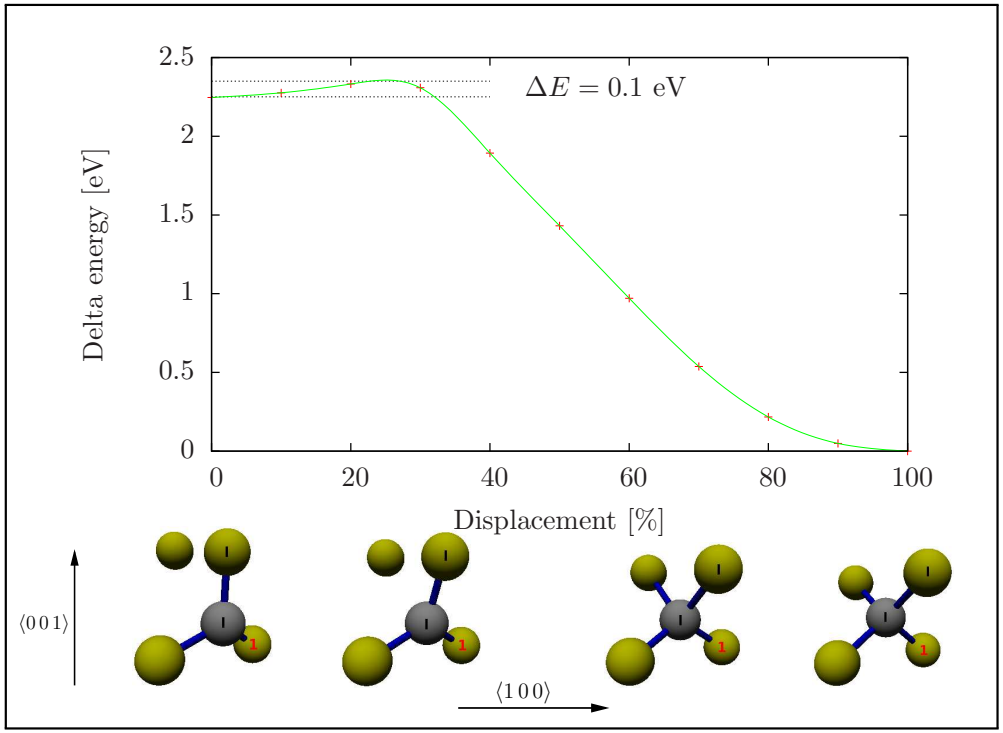

Conclusion of defect / migration / combined defect simulations

Defect structures

- Accurately described by quantum-mechanical simulations
- Less correct description by classical potential simulations

- Consistent with solubility data of C in Si
- $\langle 1\,0\,0 \rangle$ C-Si dumbbell interstitial ground state configuration
- Consistent with reorientation and diffusion experiments
- C migration pathway in Si identified

Concerning the precipitation mechanism

- Agglomeration of C-Si dumbbells energetically favorable
- C-Si indeed favored compared to C_{sub} & $\langle 1\,1\,0 \rangle$ Si self-interstitial
- Possible low interaction capture radius of C_{sub} & $\langle 1\,1\,0 \rangle$ Si self-interstitial
- In absence of nearby $\langle 1\,1\,0 \rangle$ Si self-interstitial: C-Si $\langle 1\,0\,0 \rangle$ + Vacancy $\rightarrow$ C_{sub} (SiC)

Some results point to a different precipitation mechanism!

Silicon carbide precipitation simulations

- Create c-Si volume
- Periodc boundary conditions
- Set requested T and $p = 0$ bar
- Equilibration of E_{kin} and E_{pot}

Insertion of C atoms at constant T

- total simulation volume
- volume of minimal SiC precipitate
- volume consisting of Si atoms to form a minimal precipitate

Run for 100 ps followed by cooling down to 20 °C

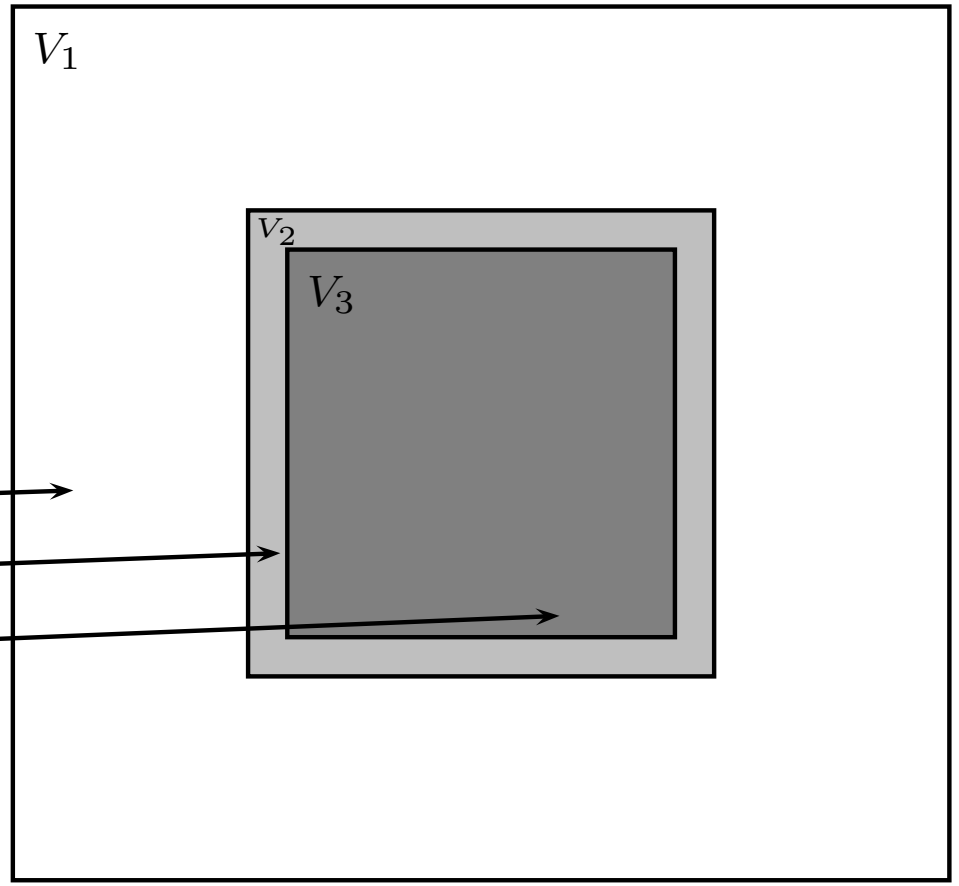

- Restricted to classical potential simulations
- V_2 and V_3 considered due to low diffusion
- Amount of C atoms: 6000 ($r_{\text{prec}} \approx 3.1$ nm, IBS: 2 ... 4 nm)
- Simulation volume: $31 \times 31 \times 31$ unit cells (238328 Si atoms)

Silicon carbide precipitation simulations at 450 °C as in IBS

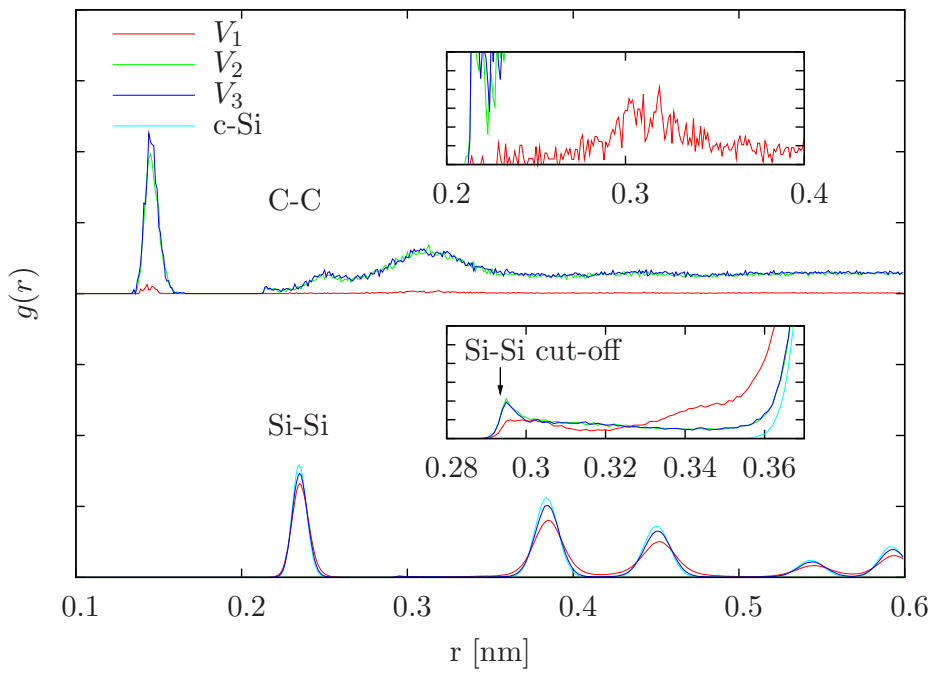

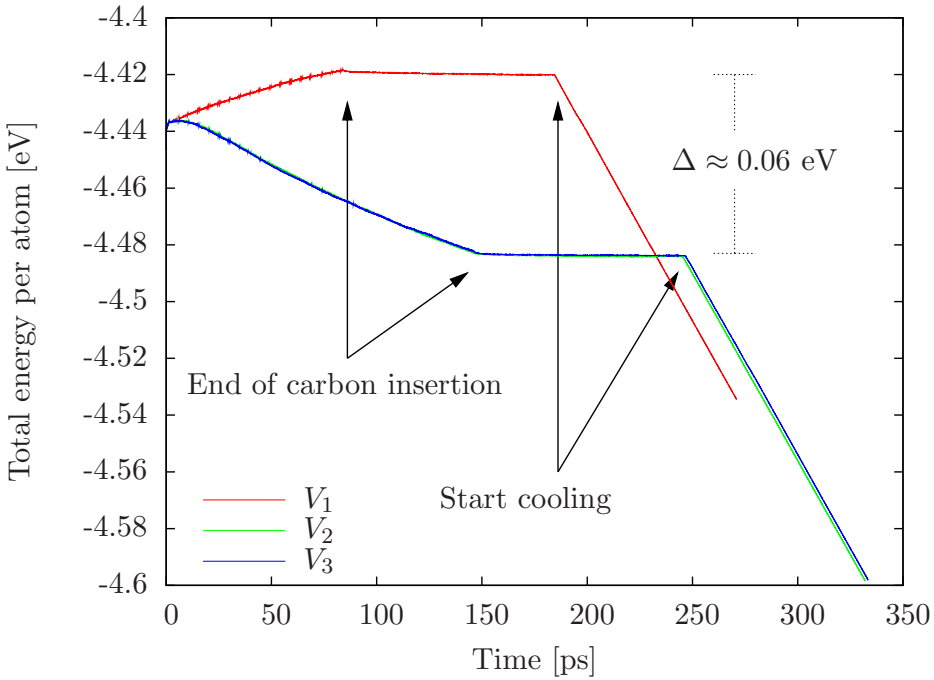

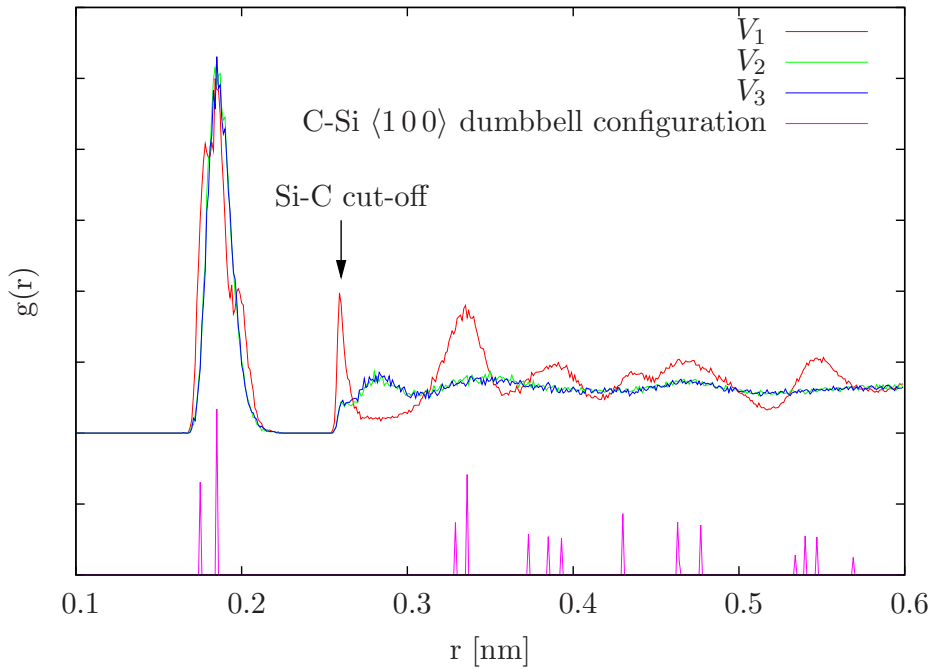

Low C concentration (V_1)

⟨1 0 0⟩ C-Si dumbbell dominated structure

- Si-C bumbs around 0.19 nm
- C-C peak at 0.31 nm (as expected in 3C-SiC): concatenated dumbbells of various orientation
- Si-Si NN distance stretched to 0.3 nm

⇒ C atoms in proper 3C-SiC distance first

High C concentration (V_2, V_3)

High amount of strongly bound C-C bonds

Defect density ↑ ⇒ considerable amount of damage

Only short range order observable

⇒ amorphous SiC-like phase

Limitations of molecular dynamics and short range potentials

Time scale problem of MD

Minimize integration error
⇒ discretization considerably smaller than reciprocal of fastest vibrational mode

Order of fastest vibrational mode: $10^{13} - 10^{14}$ Hz
⇒ suitable choice of time step: $\tau = 1$ fs $= 10^{-15}$ s
⇒ slow phase space propagation

Several local minima in energy surface separated by large energy barriers
⇒ transition event corresponds to a multiple of vibrational periods
⇒ phase transition made up of many infrequent transition events

Accelerated methods: Temperature accelerated MD (TAD), self-guided MD ...

retain proper thermodynmic sampling

Limitations related to the short range potential

Cut-off function pushing forces and energies to zero between 1^{st} and 2^{nd} next neighbours
⇒ overestimated unphysical high forces of next neighbours

Potential enhanced problem of slow phase space propagation

Approach to the (twofold) problem

Increased temperature simulations without TAD corrections
(accelerated methods or higher time scales exclusively not sufficient)

IBS

- 3C-SiC also observed for higher T
- higher T inside sample
- structural evolution vs. equilibrium properties

Increased temperature simulations at low C concentration

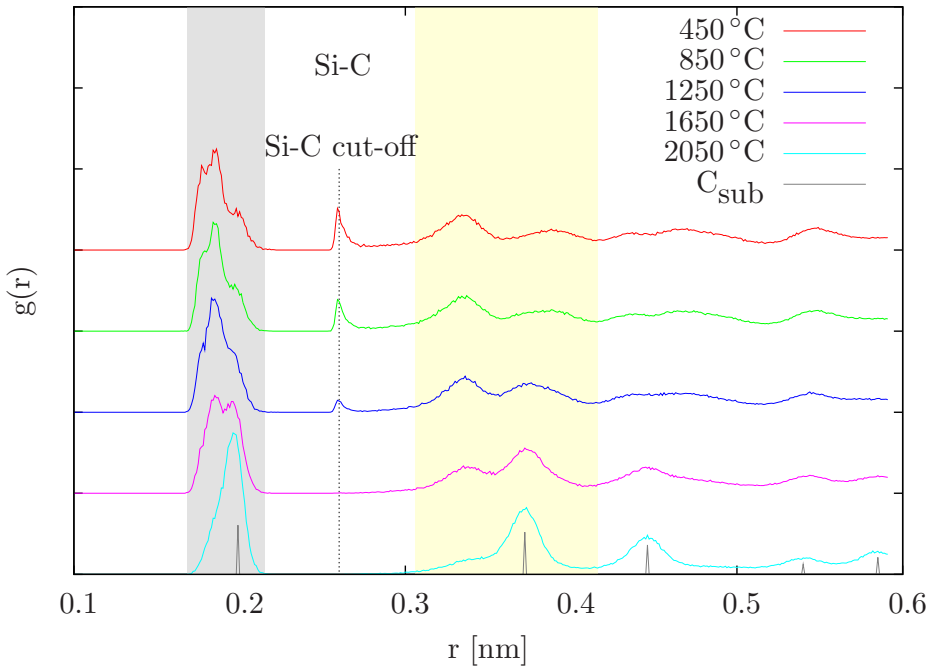

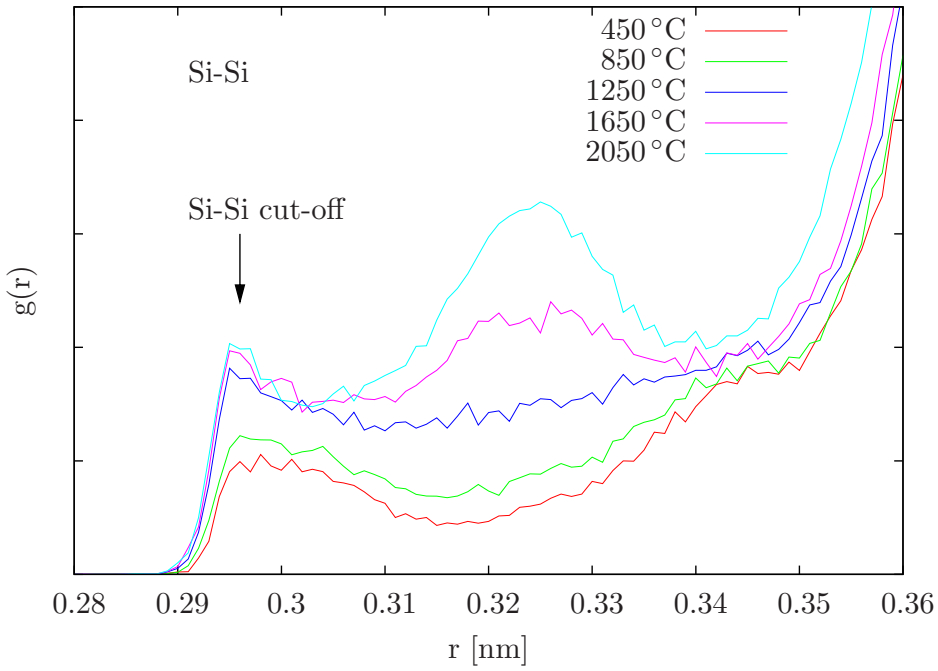

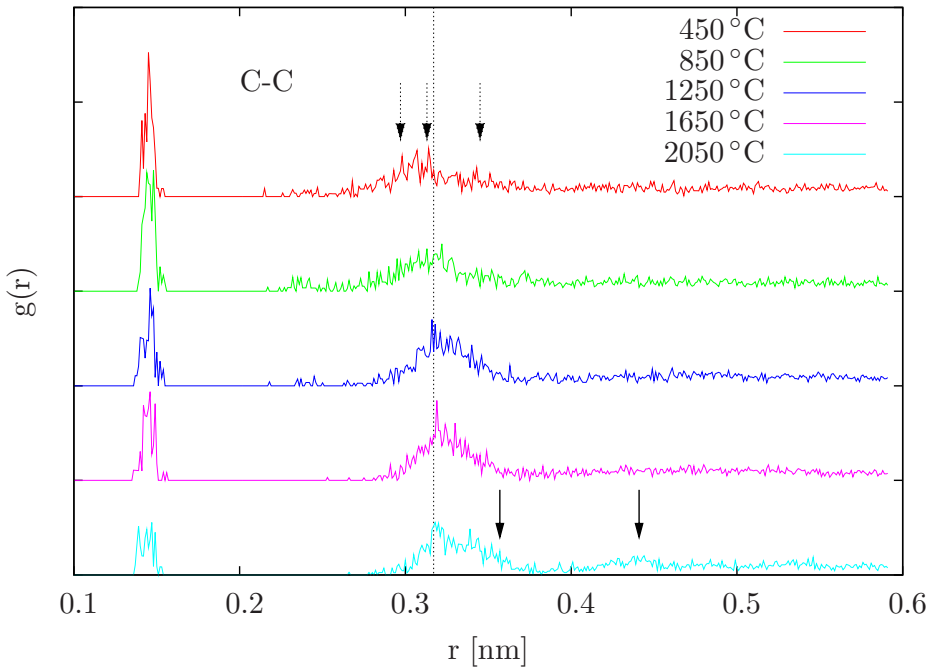

Si-C bonds:

- Vanishing cut-off artifact (above 1650 °C)
- Structural change: C-Si $\langle 1\,0\,0 \rangle \rightarrow C_{sub}$

Si-Si bonds: Si-C_{sub}-Si along $\langle 1\,1\,0 \rangle$ ($\rightarrow$ 0.325 nm)

stretched SiC in c-Si

C-C bonds:

- C-C next neighbour pairs reduced (mandatory)
- Peak at 0.3 nm slightly shifted
  - C-Si $\langle 1\,0\,0 \rangle$ combinations (dashed arrows)
    $\rightarrow$ C-Si $\langle 1\,0\,0 \rangle$ & C_{sub} combinations (|)
    $\rightarrow$ pure C_{sub} combinations (↓)
  - Range [|-↓]: C_{sub} & C_{sub} with nearby Si_I

Increased temperature simulations at high C concentration

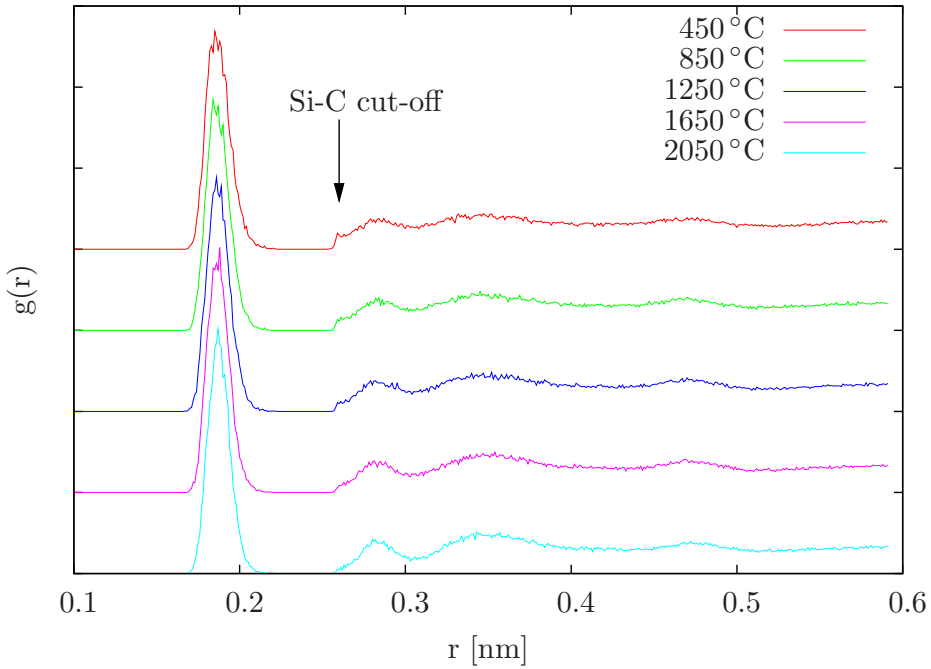

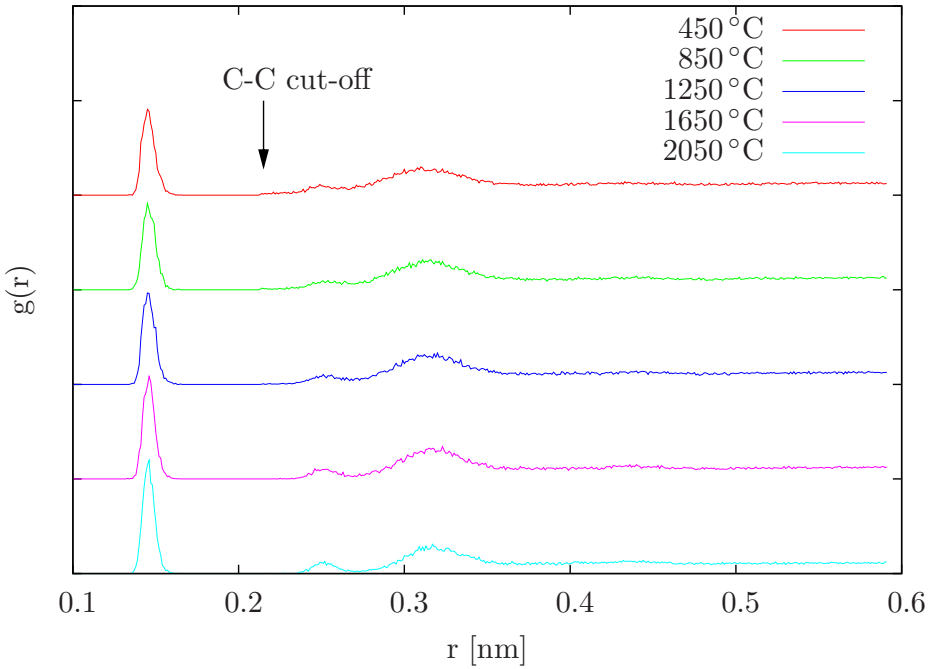

Decreasing cut-off artifact

High amount of damage & alignement to c-Si host matrix lost ⇒ hard to categorize

0.186 nm: Si-C pairs ↑ (as expected in 3C-SiC)	0.15 nm: C-C pairs ↑ (as expected in graphite/diamond)
0.282 nm: Si-C-C	0.252 nm: C-C-C (2^{nd} NN for diamond)
≈0.35 nm: C-Si-Si	0.31 nm: shifted towards 0.317 nm → C-Si-C

Amorphous SiC-like phase remains

Slightly sharper peaks ⇒ indicate slight acceleration of dynamics due to temperature

Continue with higher temperatures and longer time scales

Valuation of a practicable temperature limit

Recrystallization is a hard task! ⇒ Avoid melting!

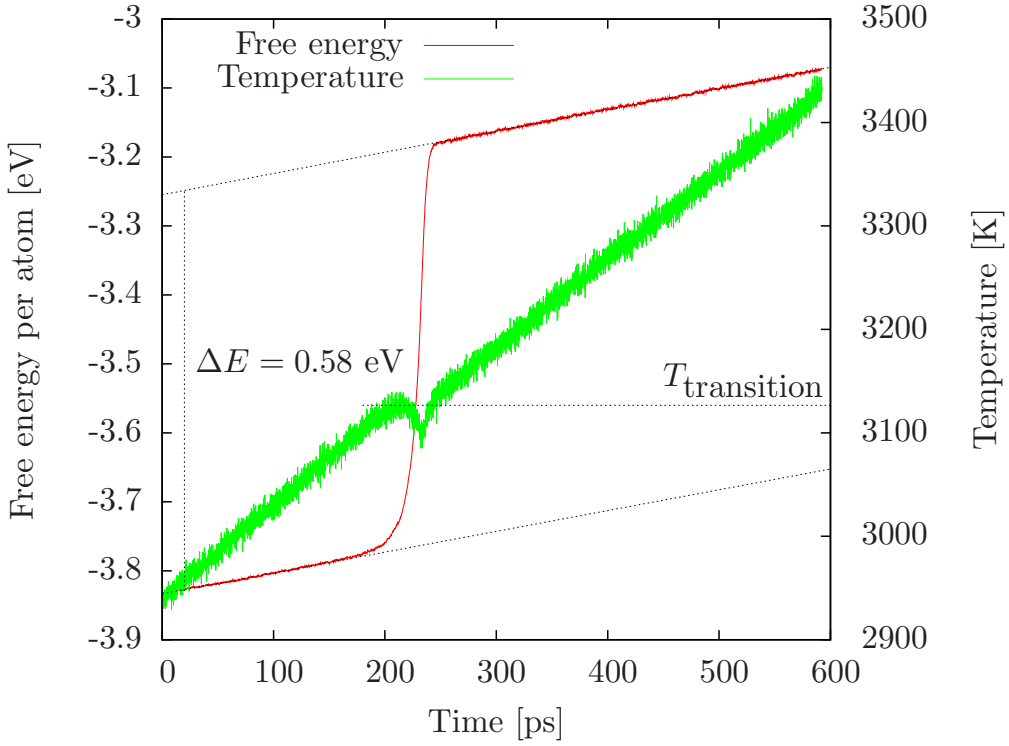

Melting does not occur instantly after exceeding the melting point $T_{\text{m}} = 2450$ K

- required transition enthalpy
- hysterisis behaviour

Heating up c-Si by 1 K/ps

- transition occurs at ≈ 3125 K
- $\Delta E = 0.58$ eV/atom $= 55.7$ kJ/mole (literature: 50.2 kJ/mole)

Initially chosen temperatures:
$1.0 - 1.2 \cdot T_{\text{m}}$

$\Longrightarrow$

Introduced C (defects)
→ reduction of transition point
→ melting already at T_{m}

Maximum temperature used: $0.95 \cdot T_{\text{m}}$

Long time scale simulations at maximum temperature

Differences

- Temperature set to $0.95 \cdot T_{\mathrm{m}}$
- Cubic insertion volume $\Rightarrow$ spherical insertion volume
- Amount of C atoms: 6000 $\rightarrow$ 5500 $\Leftrightarrow r_{\mathrm{prec}} = 0.3$ nm
- Simulation volume: 21 unit cells of c-Si in each direction

Low C concentration, Si-C

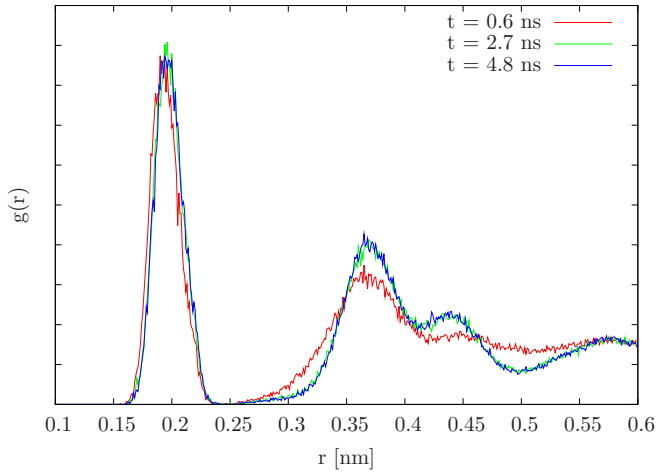

Sharper peaks!

Low C concentration, C-C

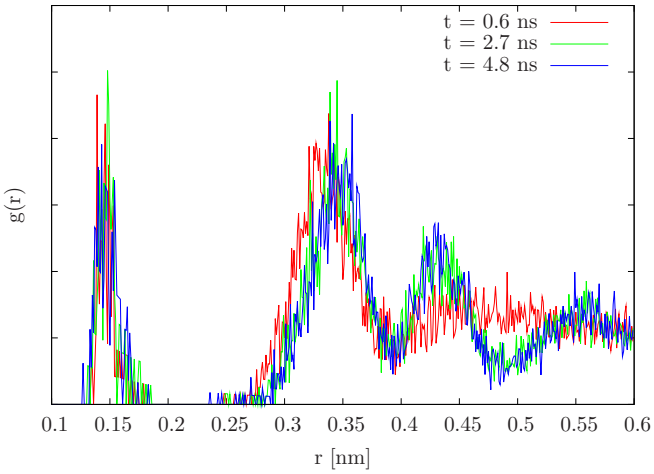

Sharper peaks!

No C agglomeration!

High C concentration

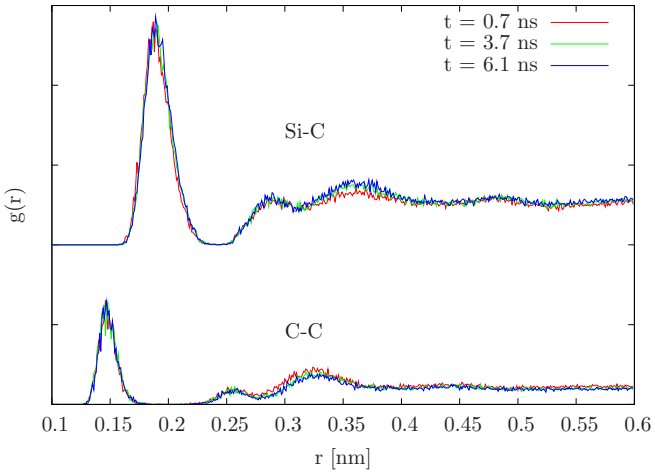

No significant changes

Long time scales and high temperatures most probably not sufficient enough!

Investigation of a silicon carbide precipitate in silicon

$$\frac{8}{a_{\mathrm{Si}}^3}\Big(\underbrace{21^3 a_{\mathrm{Si}}^3}_{=V} - \frac{4}{3}\pi x^3\Big) + \underbrace{\frac{4}{y^3}\frac{4}{3}\pi x^3}_{\stackrel{!}{=}5500} = 21^3 \cdot 8$$

$$\Downarrow$$

$$\frac{8}{a_{\mathrm{Si}}^3}\frac{4}{3}\pi x^3 = 5500 \Rightarrow x = \left(\frac{5500 \cdot 3}{32\pi}\right)^{1/3} a_{\mathrm{Si}}$$

$$y = \left(\frac{1}{2}\right)^{1/3} a_{\mathrm{Si}}$$

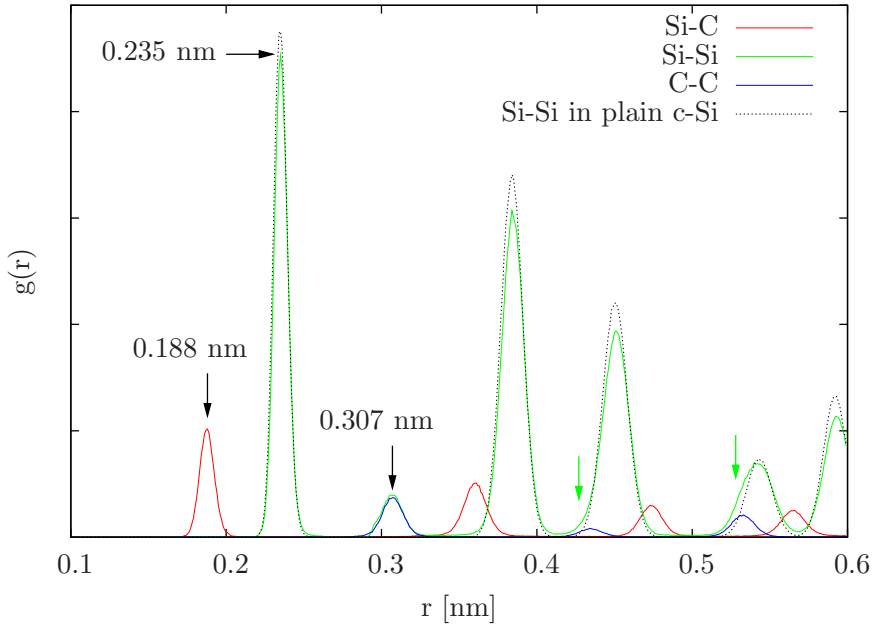

Construction

- Simulation volume: 21^3 unit cells of c-Si
- Spherical topotactically aligned precipitate
  $r = 3.0$ nm $\Leftrightarrow \approx 5500$ C atoms
- Create c-Si but skipped inside sphere of radius x
- Create 3C-SiC inside sphere of radius x
  and lattice constant y
- Strong coupling to heat bath ($T = 20\,^\circ$C)

Results

- Slight increase of c-Si lattice constant!
- C-C peaks (imply same distanced Si-Si peaks)
  - New peak at 0.307 nm: 2^{nd} NN in 3C-SiC
  - Bumps (↓): 4^{th} and 6^{th} NN
- 3C-SiC lattice constant: 4.34 Å(bulk: 4.36 Å)
  → compressed precipitate
- Interface tension:
  20.15 eV/nm^2 or 3.23×10^{-4} J/cm^2
  (literature: $2 - 8 \times 10^{-4}$ J/cm^2)

Investigation of a silicon carbide precipitate in silicon

Appended annealing steps

- artificially constructed interface
  → allow for rearrangement of interface atoms
- check SiC stability

Temperature schedule

- rapidly heat up structure up to 2050 °C
  (75 K/ps)
- slow heating up to $1.2 \cdot T_\mathrm{m} = 2940$ K by 1 K/ps
  → melting at around 2840 K (▷)
- cooling down structure at 100 % T_m (1 K/ps)
  → no energetically more favorable struture

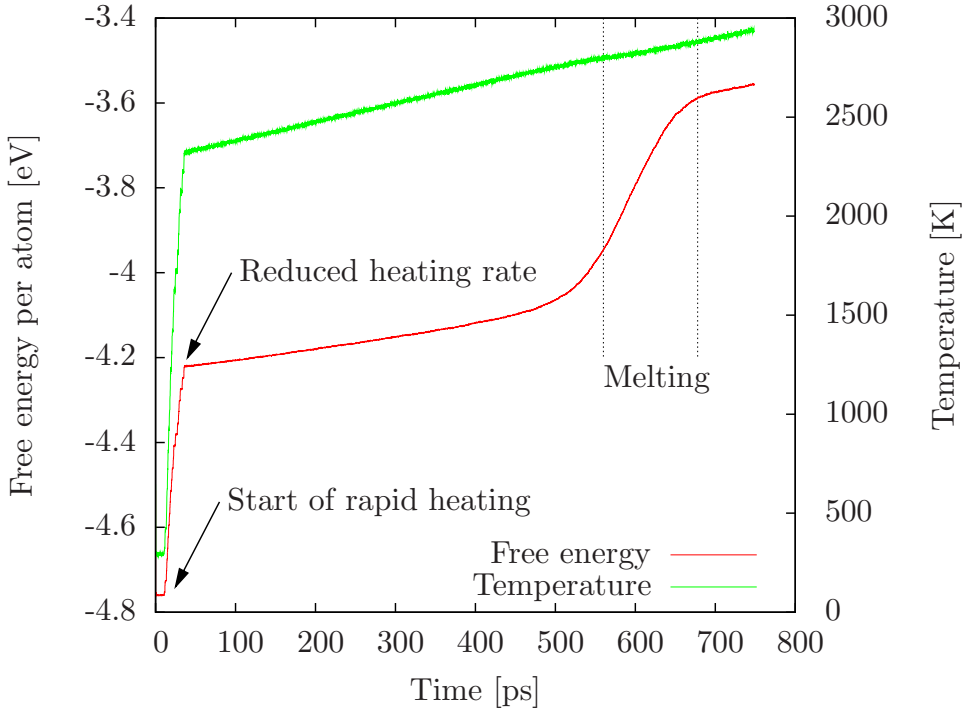

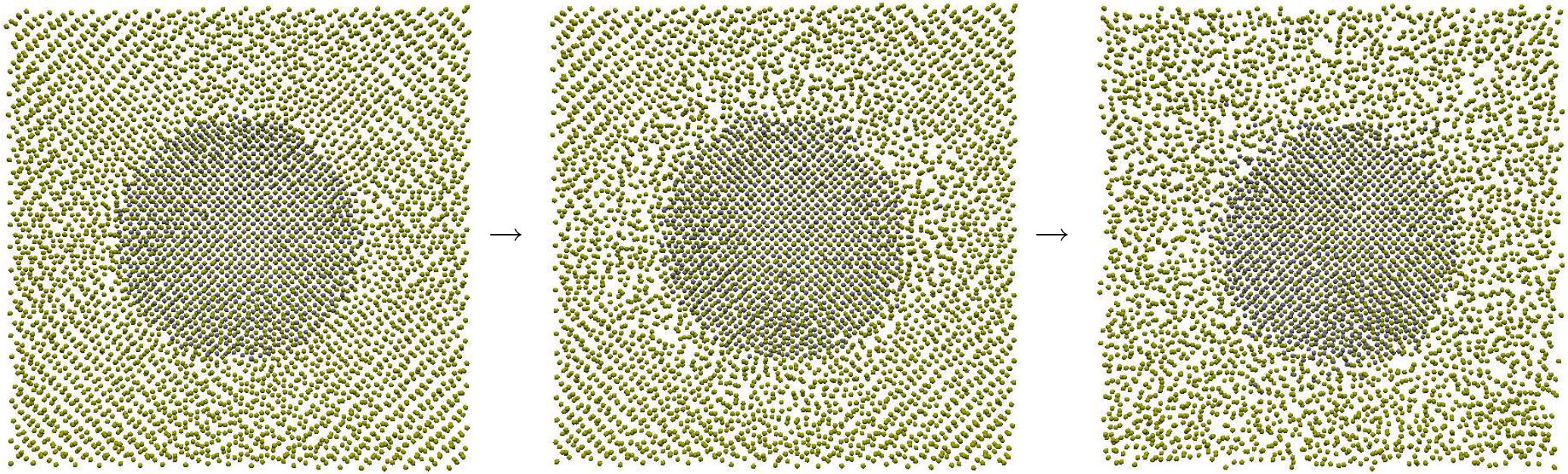

Summary / Conclusion / Outlook

Defects

- Summary & conclusion
  - Point defects excellently / fairly well described by QM / classical potential simulations
  - Identified migration path explaining diffusion and reorientation experiments
  - Agglomeration of point defects energetically favorable
  - C_{sub} favored conditions (conceivable in IBS)
- Todo
  - Discussions concerning interpretation of QM results (Paderborn)
  - Compare migration barrier of $\langle 1\,1\,0 \rangle$ Si and C-Si $\langle 1\,0\,0 \rangle$ dumbbell
  - Combination: Vacancy & $\langle 1\,1\,0 \rangle$ Si self-interstitial & C-Si $\langle 1\,0\,0 \rangle$ dumbbell (IBS)

Pecipitation simulations

- Summary & conclusion
  - Low T $\rightarrow$ C-Si $\langle 1\,0\,0 \rangle$ dumbbell dominated structure
  - High T $\rightarrow$ C_{sub} dominated structure
  - High C concentration $\rightarrow$ amorphous SiC like phase
- Todo
  - Accelerated method: self-guided MD
  - Activation relaxation technique
  - Constrainted transition path

Constructed 3C-SiC precipitate

- Summary & conclusion
  - Small / stable / compressed 3C-SiC precipitate in slightly stretched c-Si matrix
  - Interface tension matches experiemnts
- Todo
  - Try to improve interface
  - Precipitates of different size

Acknowledgements

Thanks to ...

Augsburg

- Prof. B. Stritzker (accepting a simulator at EP IV)
- Ralf Utermann (EDV)

Helsinki

- Prof. K. Nordlund (MD)

Munich

- Bayerische Forschungsstiftung (financial support)

Paderborn

- Prof. J. Lindner (SiC)
- Prof. G. Schmidt (DFT + financial support)
- Dr. E. Rauls (DFT + SiC)

Thank you for your attention!